Max-Planck-Institut für Astrophysik

SFB 1258 Neutrinos Dark Matter Messengers

Excellence Cluster Universe

GW170817: The First Double Neutron Star Merger
Kavli Institute for Theoretical Physics, UCSB, Dec. 5–8, 2017

Jet Formation and Mass Ejection in Neutron-Star Mergers

Hans-Thomas Janka
Max Planck Institute for Astrophysics, Garching

Evolution Paths of NS+NS/BH Mergers

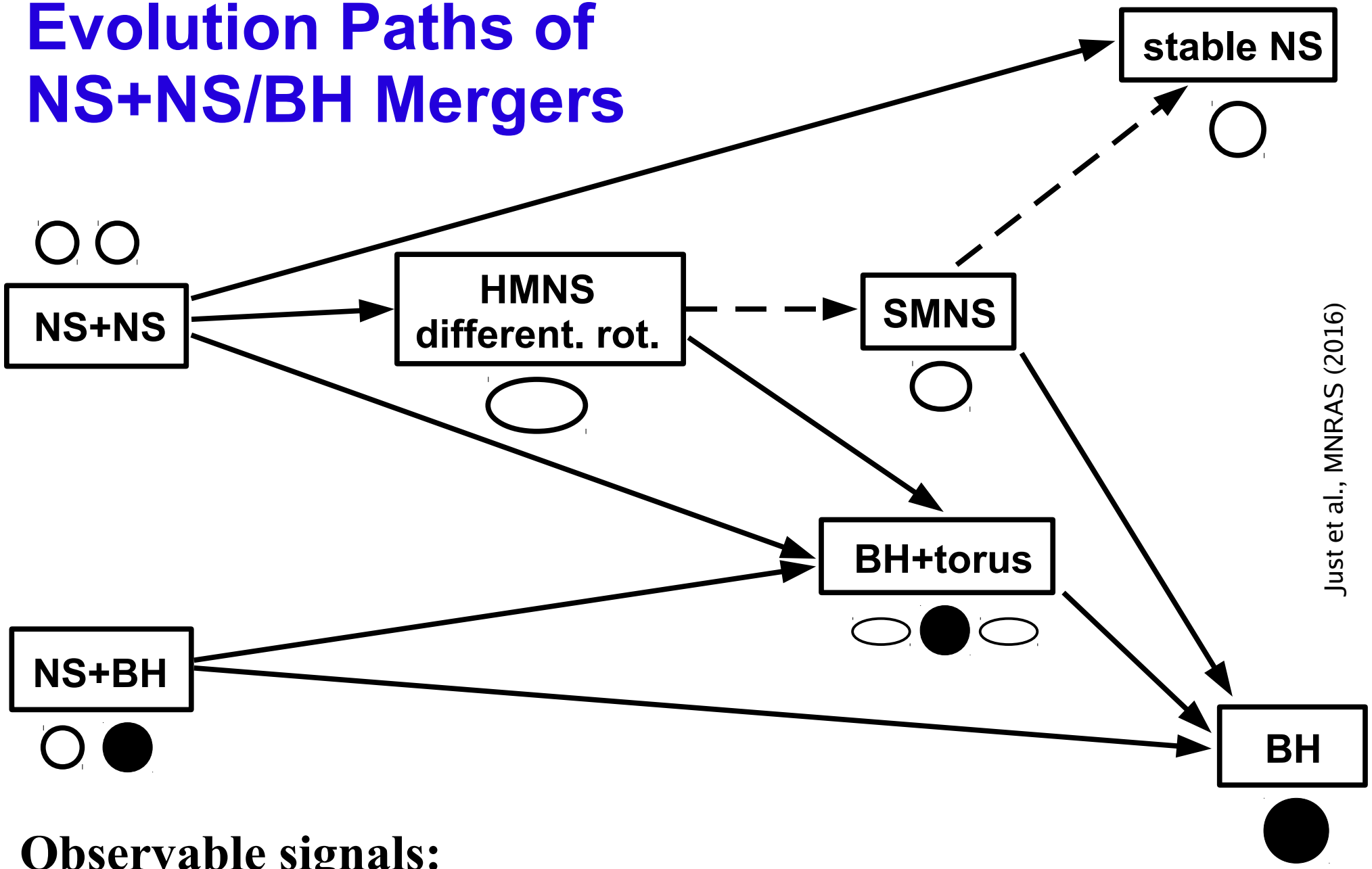

Observable signals:

Gravitational waves, neutrinos, gamma-ray bursts,
mass ejection, r-process elements, electromagnetic transients

Neutron Star Mergers as Production Sites of Ejecta & Heavy Elements

Compact binary mergers

- are likely sources of short gamma-ray bursts
  (Paczynski, Jaroszynski, etc.)
- are among strongest sources of gravitational waves
- are potential production sites of r-process nuclei
  (Lattimer & Schramm 1974, 1976; Lattimer et al. 1977; Meyer 1989, Freiburghaus et al. 1999)
- May be observable transient sources of optical radiation
  (Li & Paczynski 1998, Kulkarni 2005, Metzger et al. 2010, Roberts et al. 2011)

  and radio flares (Piran & Nakar 2011)

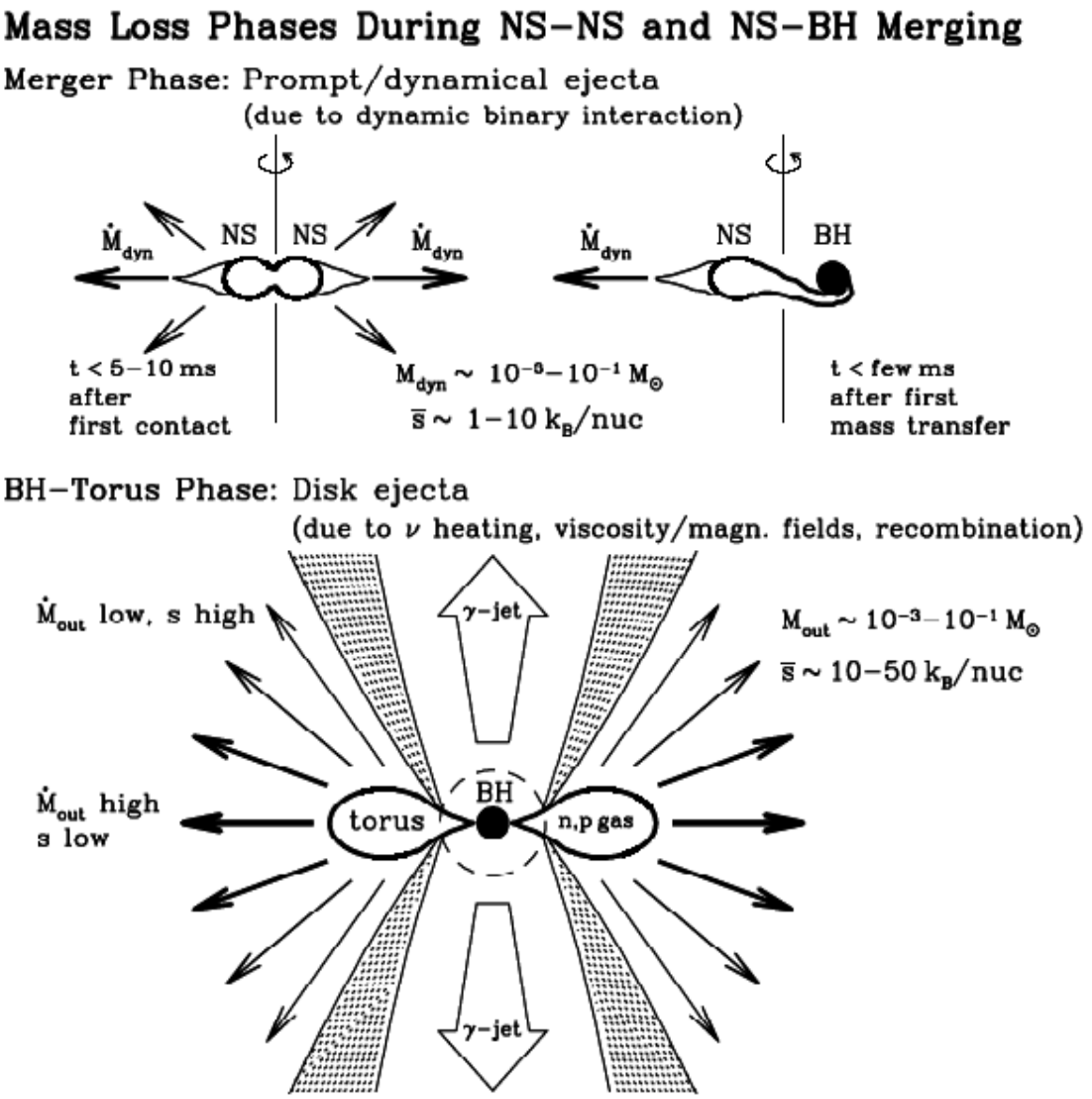

(Ruffert & Janka 1999; Just et al., MNRAS 448 (2015) 541)

Merger Remnants & GRB Central Engines

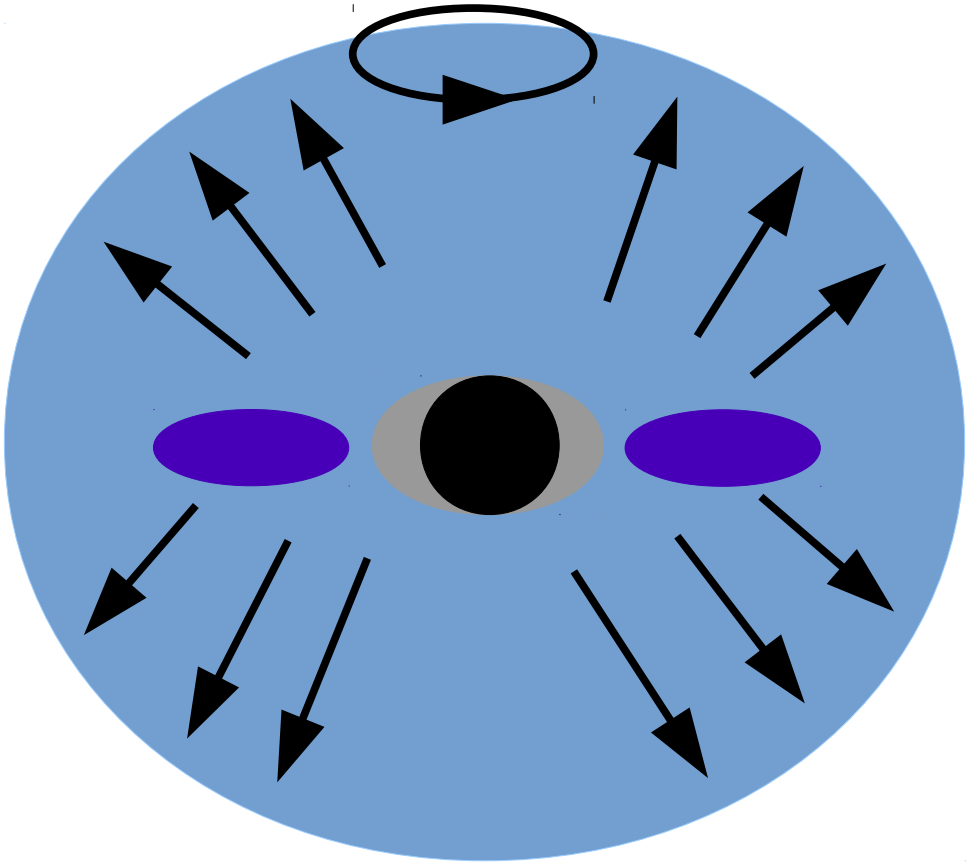

BH+torus

Blinnikov (1986), Eichler+ (1989),
Woosley (1993), etc., etc.

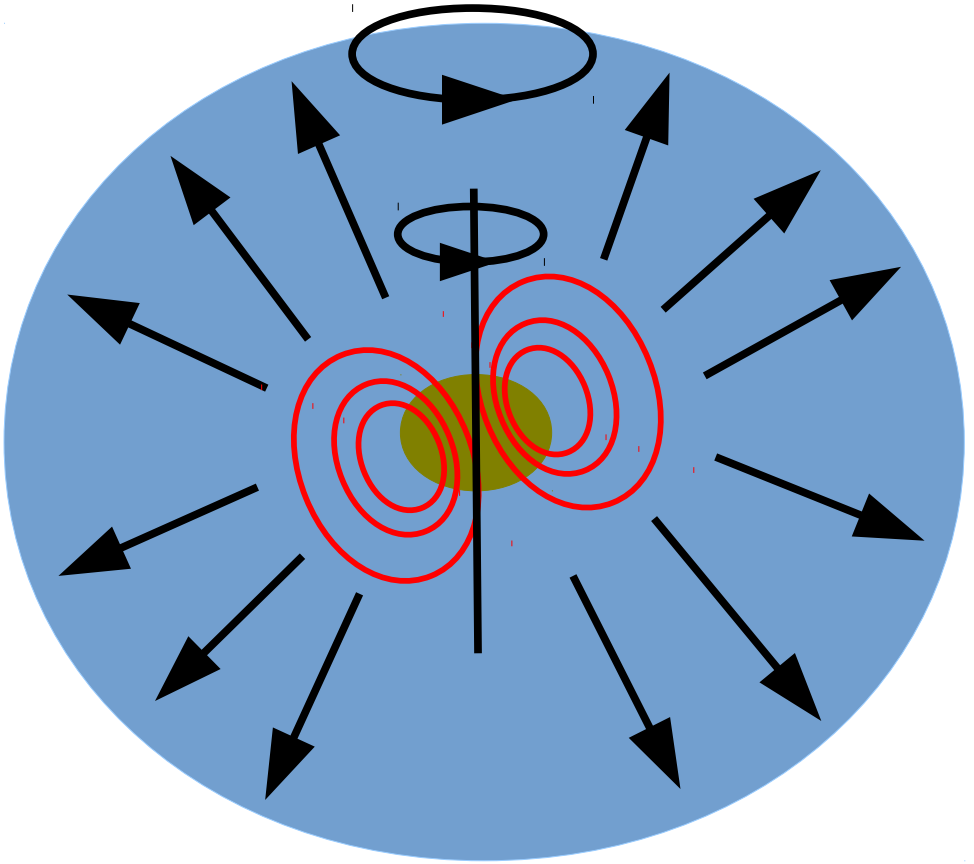

Magnetar "engine"

Usov (1992), Metzger et al. (2011),
Bucciantini et al. (2007, 2008, 2009)

Jet Formation in Compact Binary Mergers

GRB Jets From NS Mergers

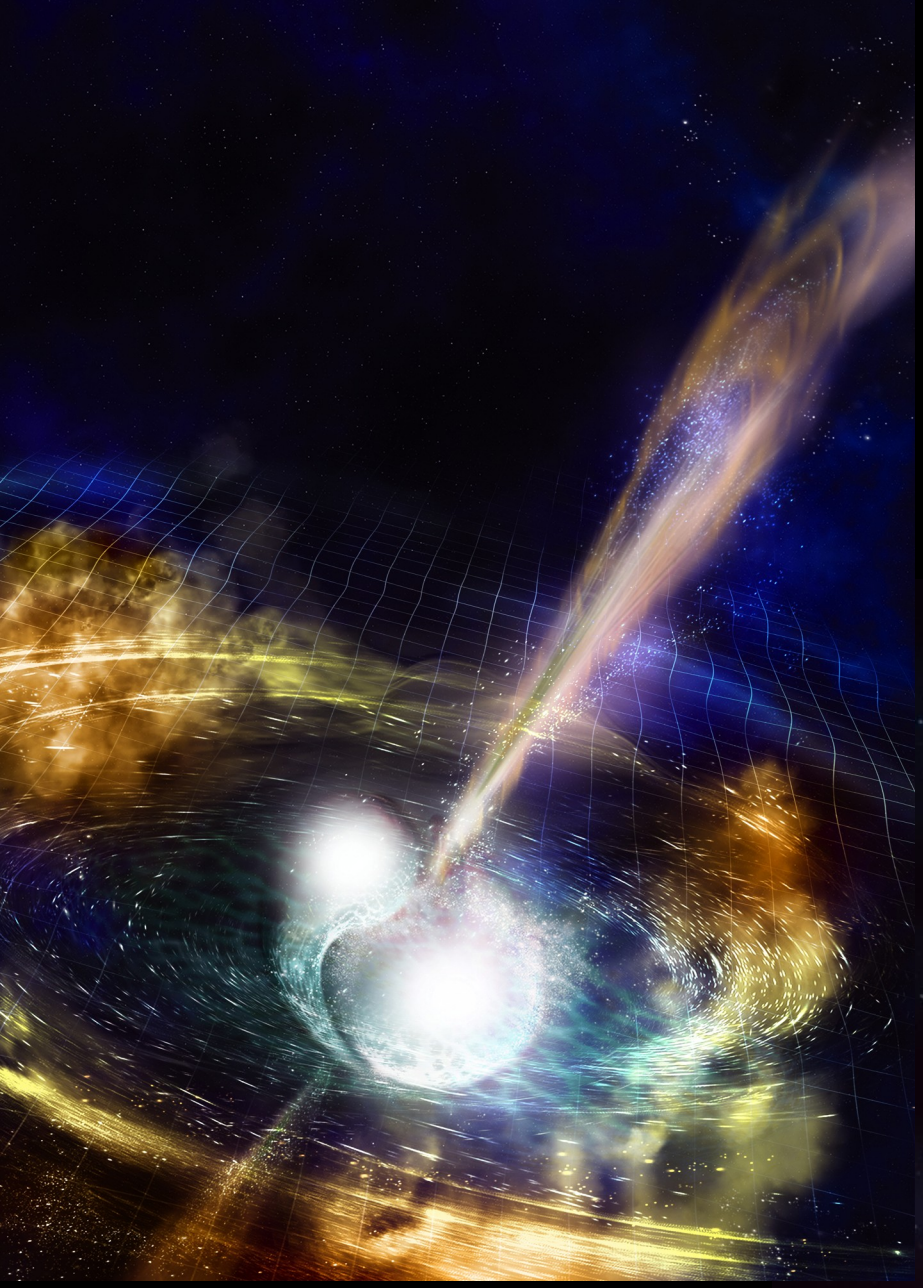

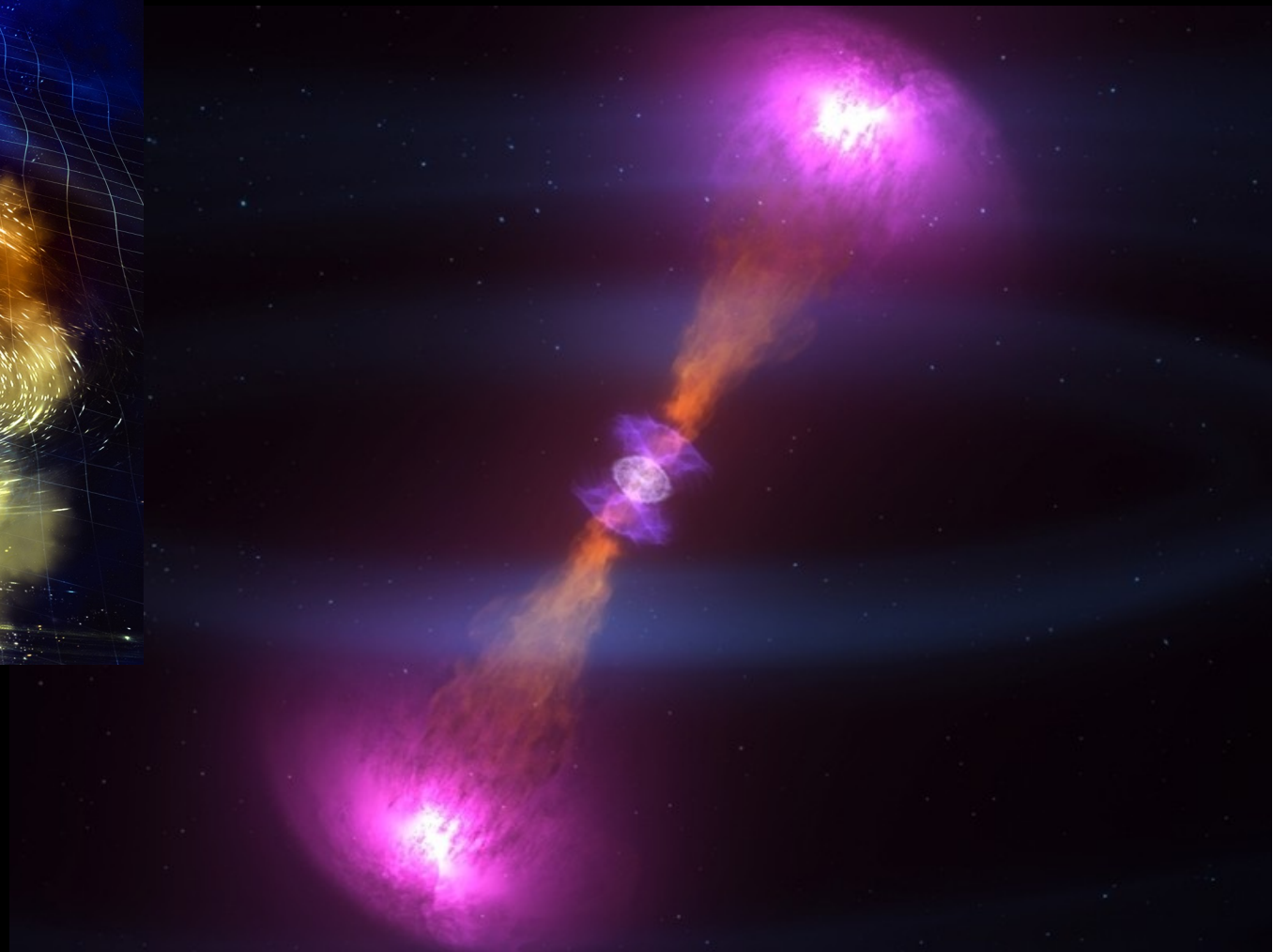

Neutrinos as energy source of ultra-relativistic, collimated outflows

$\nu + \nu \longrightarrow e^+ + e^- \longleftrightarrow \gamma + \gamma$

Pair-Plasma Fireball

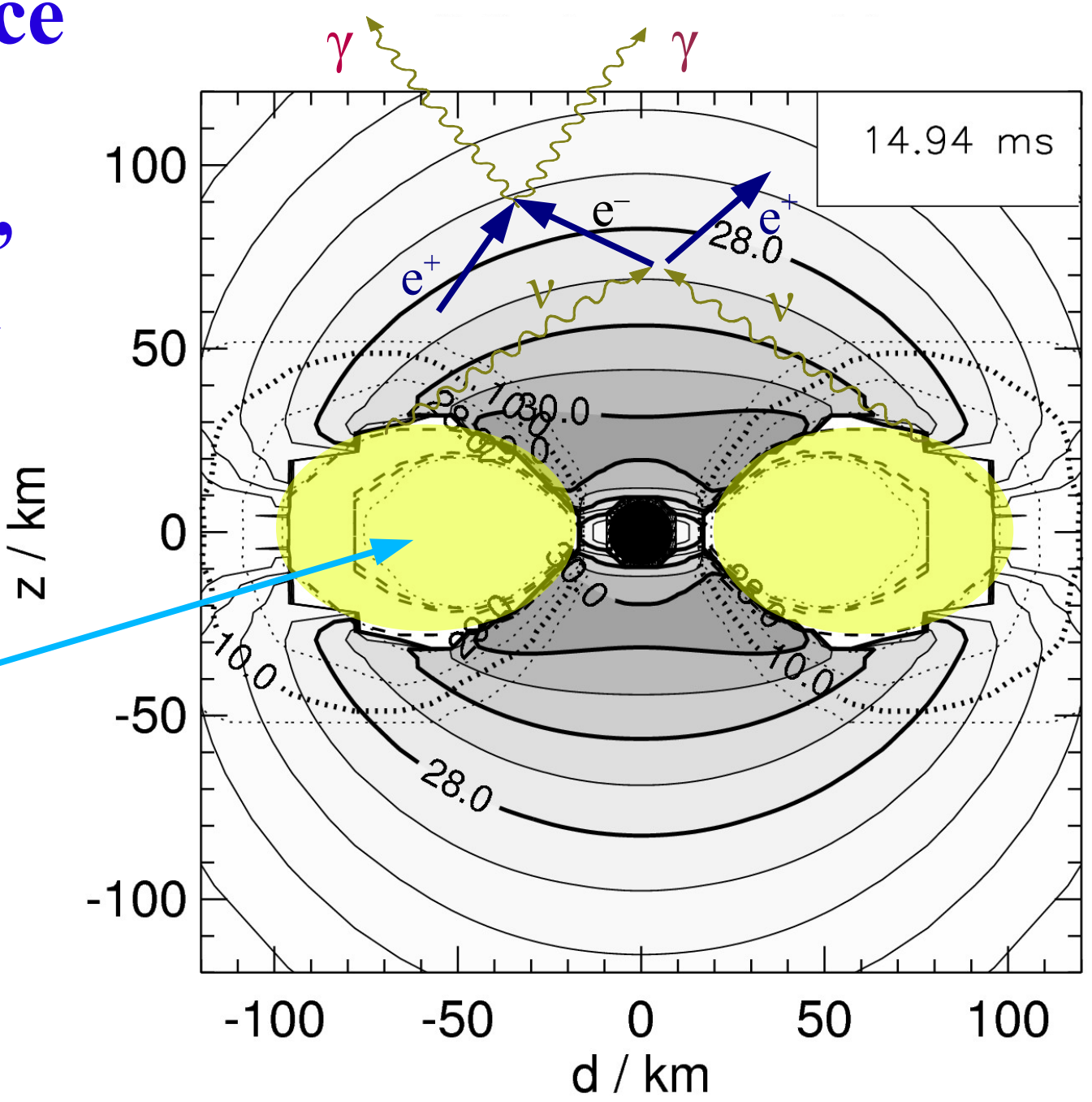

Extremely hot torus radiates high neutrino luminosities into polar low-density funnels.

Neutrino Annihilation around BH-Tori

- relic BH can accrete from massive, hot, neutrino-radiating torus
- accretion efficiency: 5–20%
- annihilation efficiency: up to a few %
- ~30% of annihilation energy deposited in low-density polar funnels (up to ~10^{50} erg)

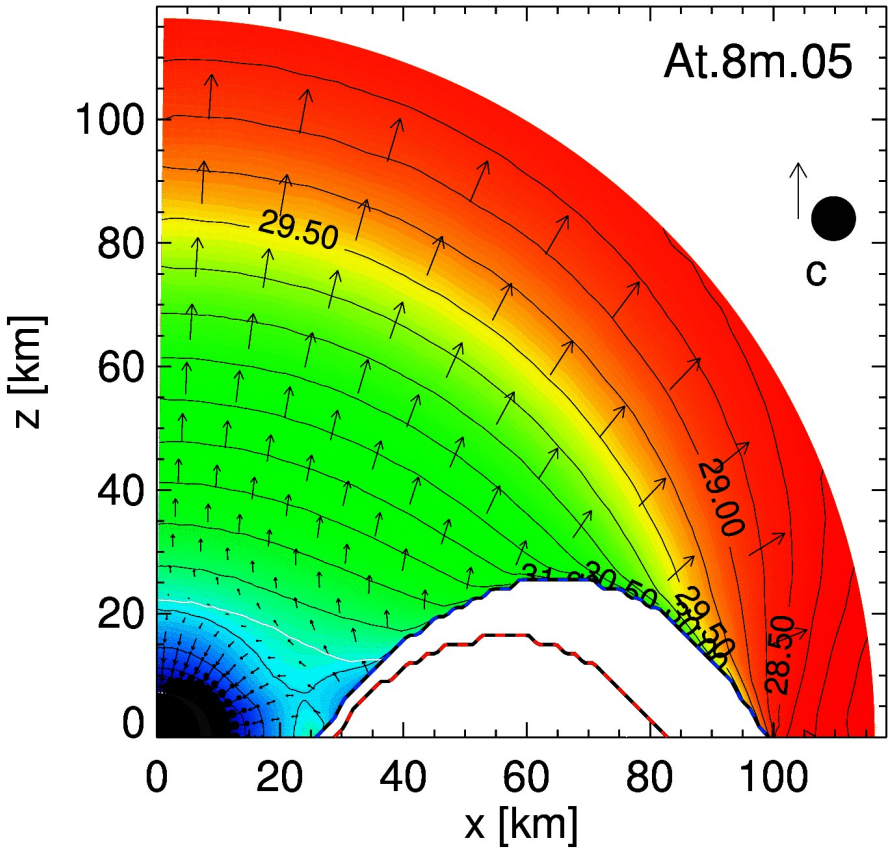

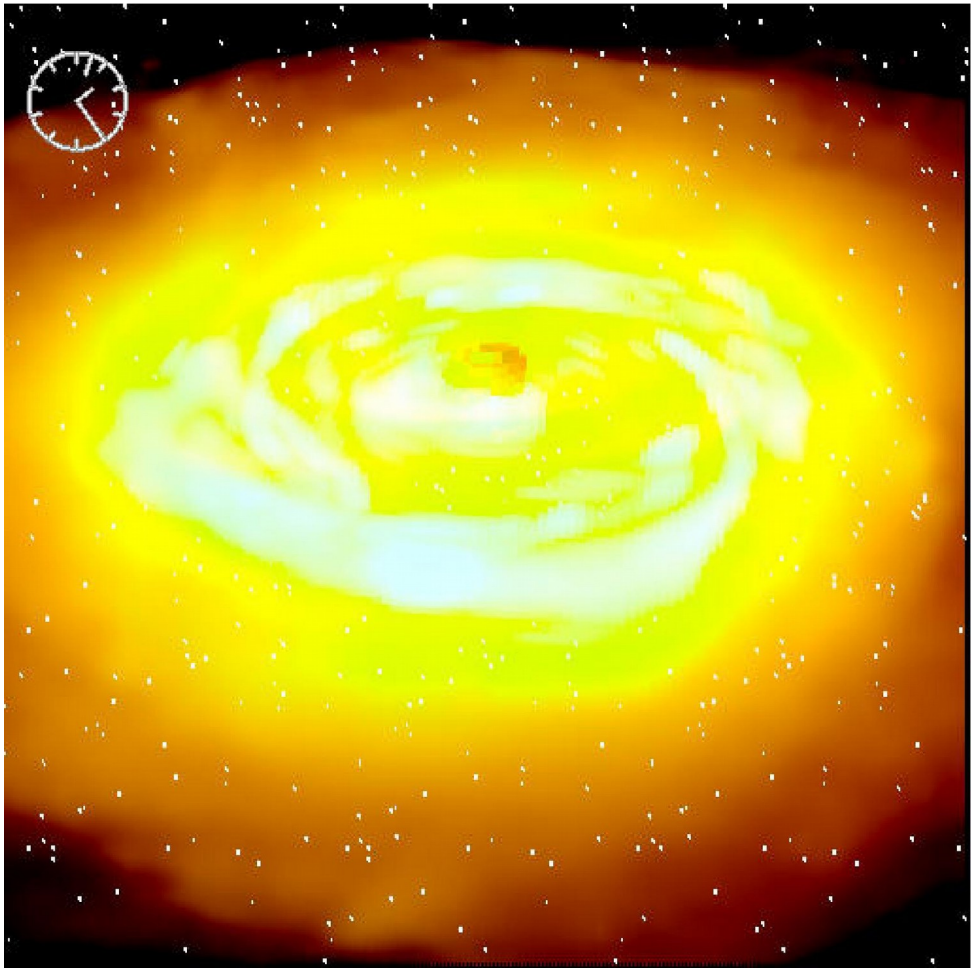

Setiawan, Ruffert, HTJ, MNRAS (2004)

Birkl, Aloy, HTJ & Müller, A&A (2007)

Relativistic Jets from BH-Tori

- General relativistic simulations of jet formation at the BH.
- Thermal energy deposition dE/dt a few 10^{50} erg/s for about 0.1 s.
- Energy deposition in axial cone with varied opening angle, decline as z^{-5}.

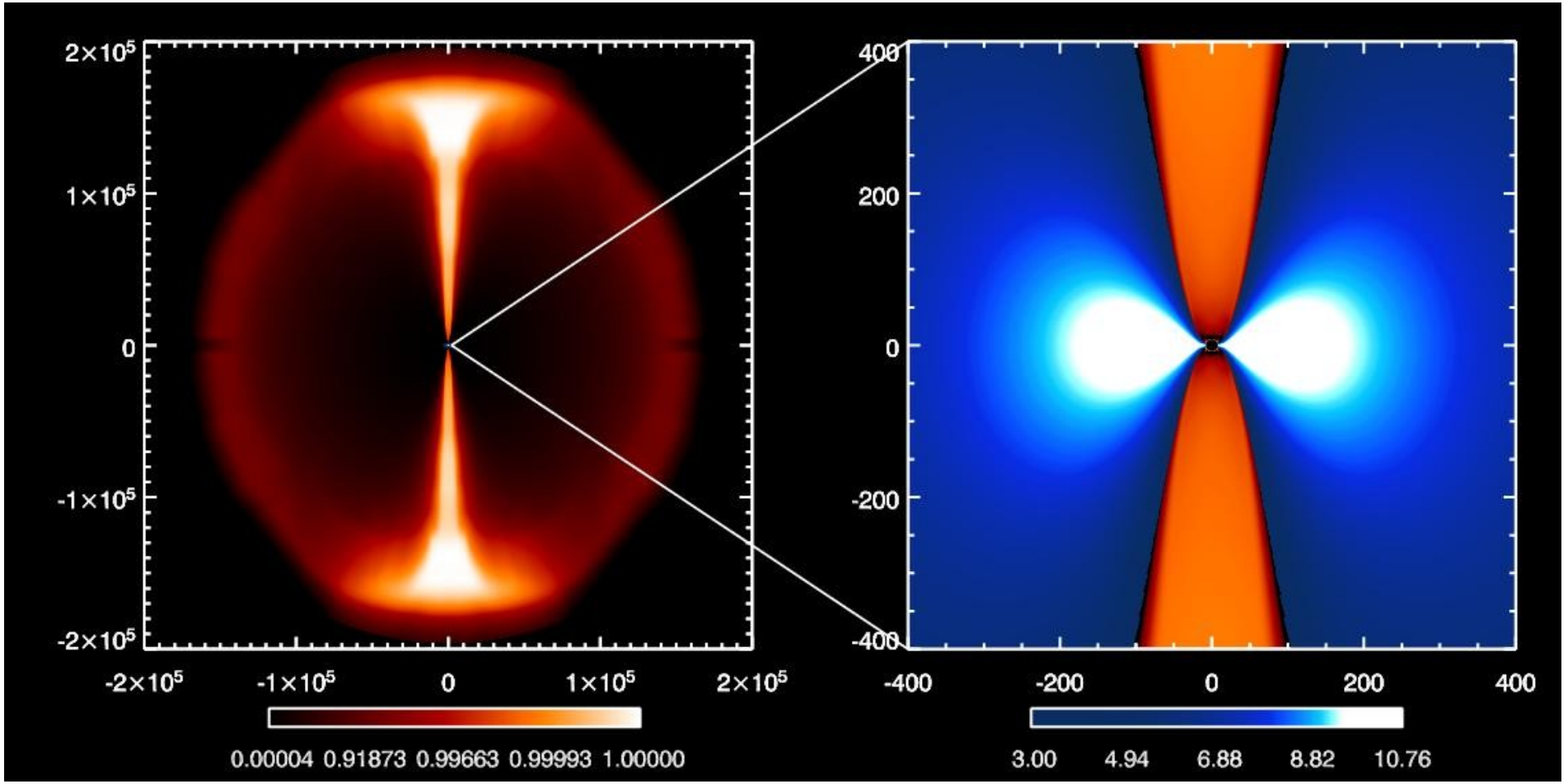

Aloy, HTJ, & Müller, A&A 436 (2005) 273

Angular Structure of Relativistic Jets from BH-Tori

- General relativistic simulations of jet formation at the BH.
- Thermal energy deposition dE/dt a few 10^{50} erg/s for about 0.1 s.
- Energy deposition in axial cone with varied opening angle, decline as z^{-5}.

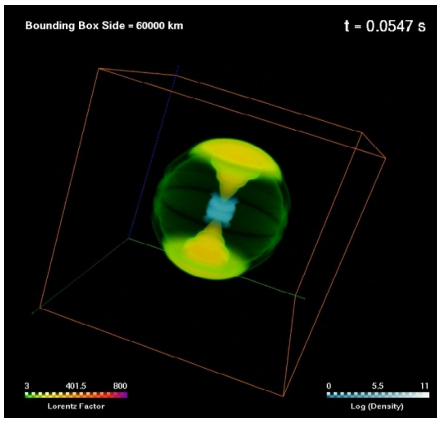

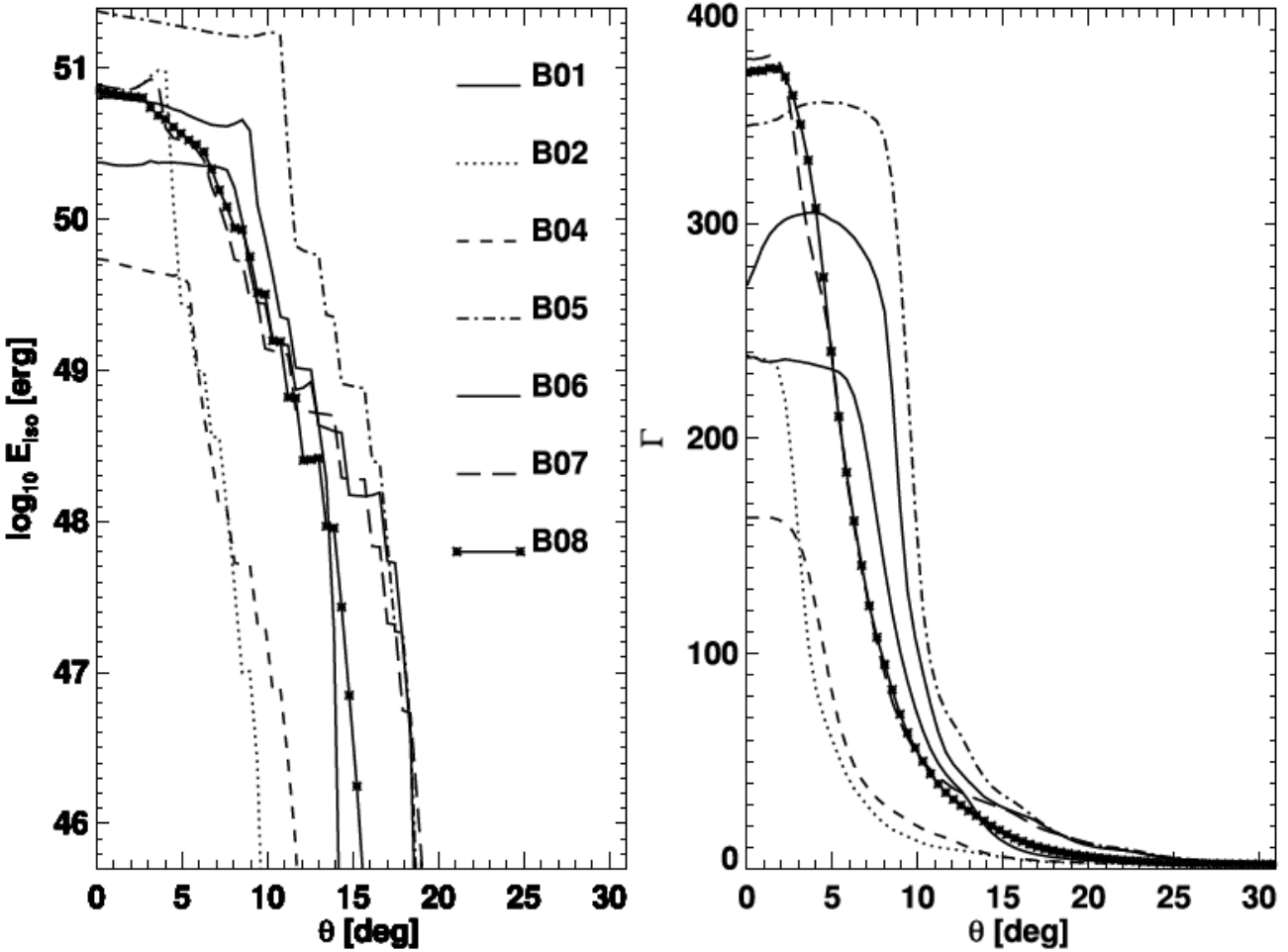

Aloy, HTJ, & Müller, A&A 436 (2005) 273; THJ et al., ApJ 654 (2006) 1305

Jets and Outflows from Compact Binary Mergers

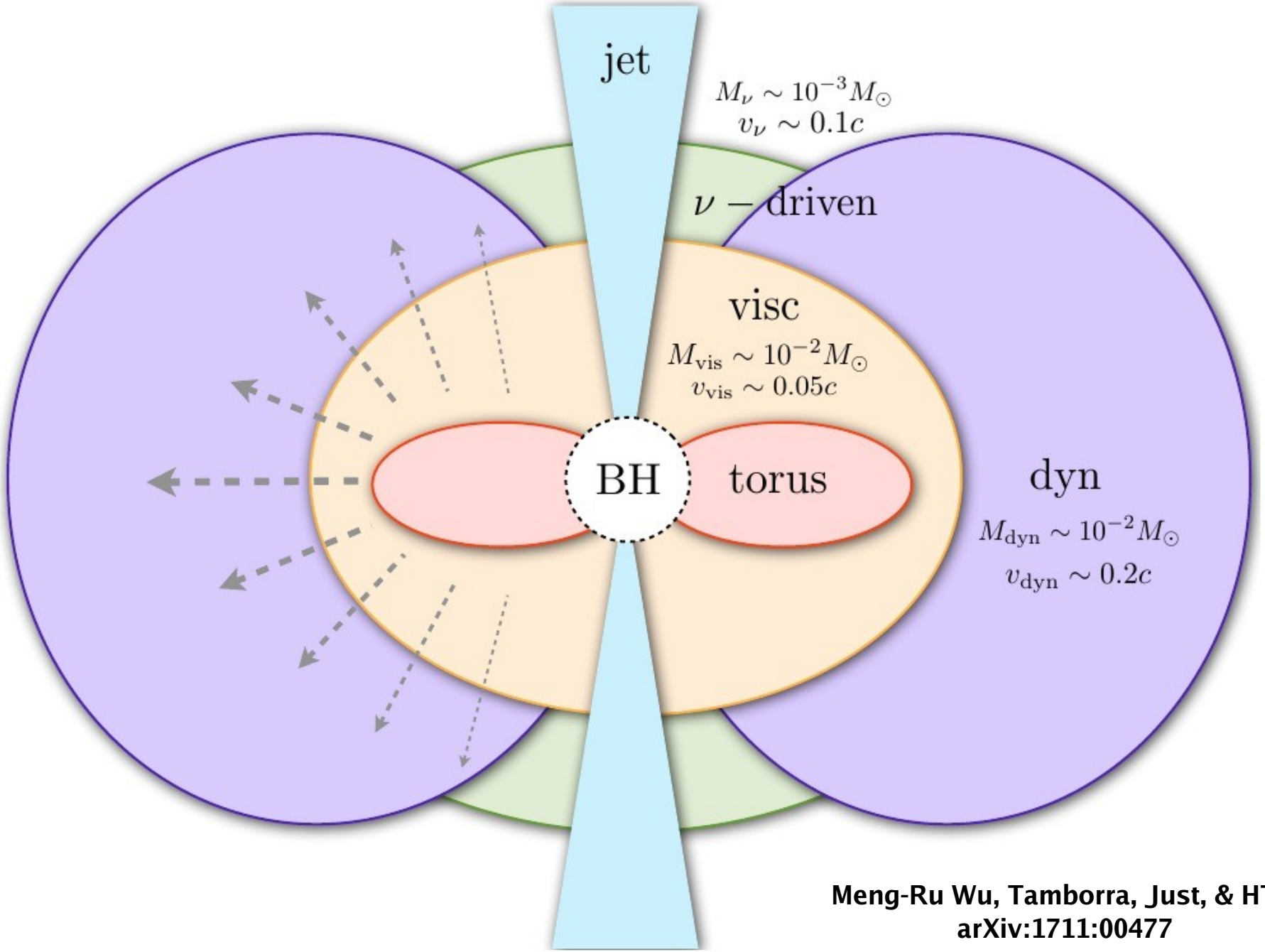

Meng-Ru Wu, Tamborra, Just, & HTJ,
arXiv:1711:00477

Structural Components of Supersonic Jets

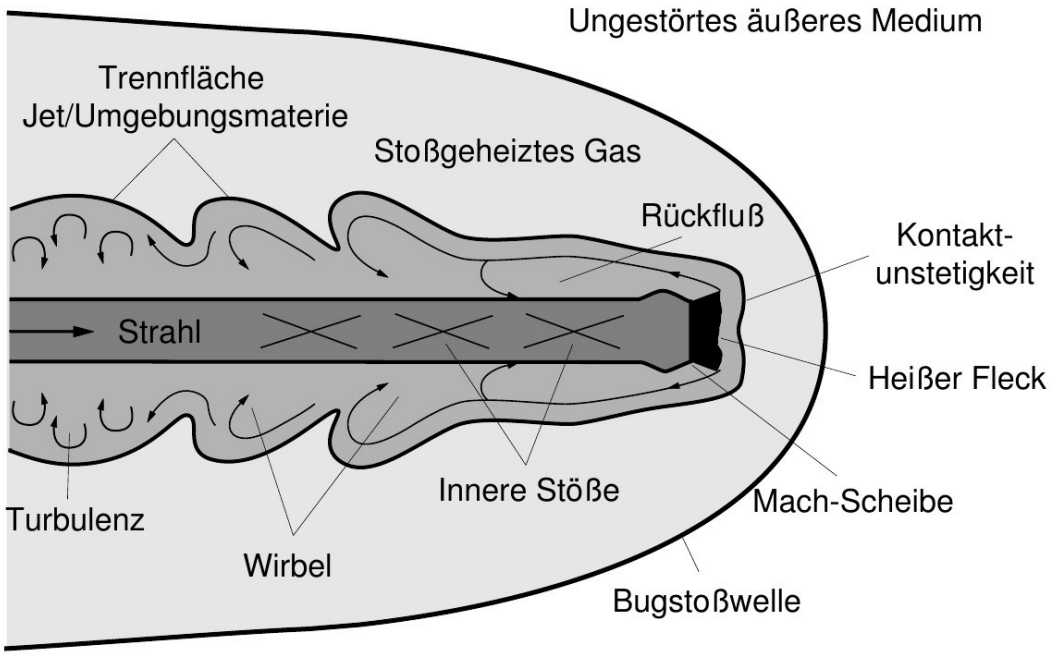

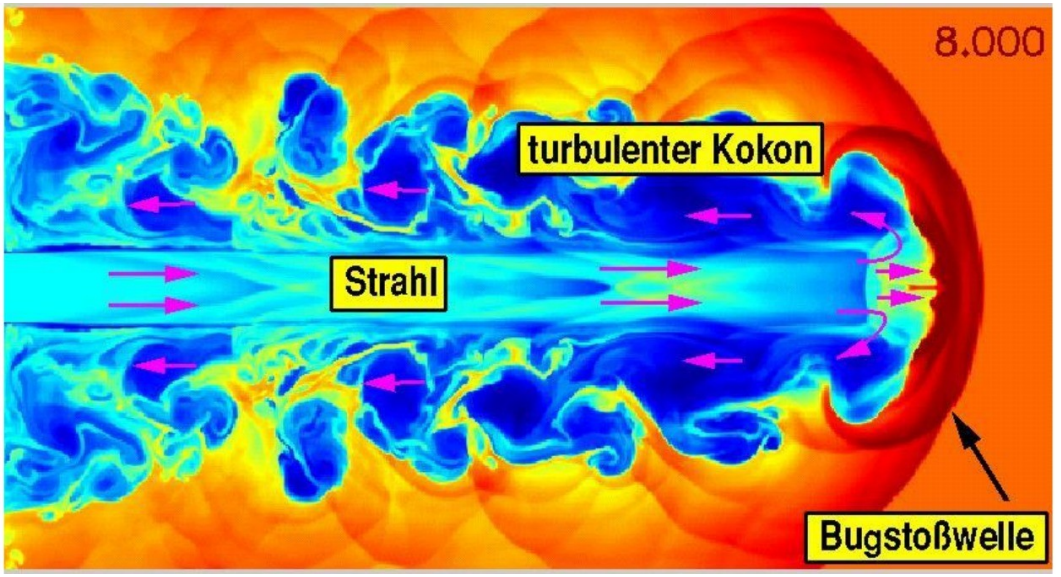

Ewald Müller,
Computational Methods for Astrophysical Fluid Flow,
Saas-Fee Advanced Course 27.
Lecture Notes 1997, Springer

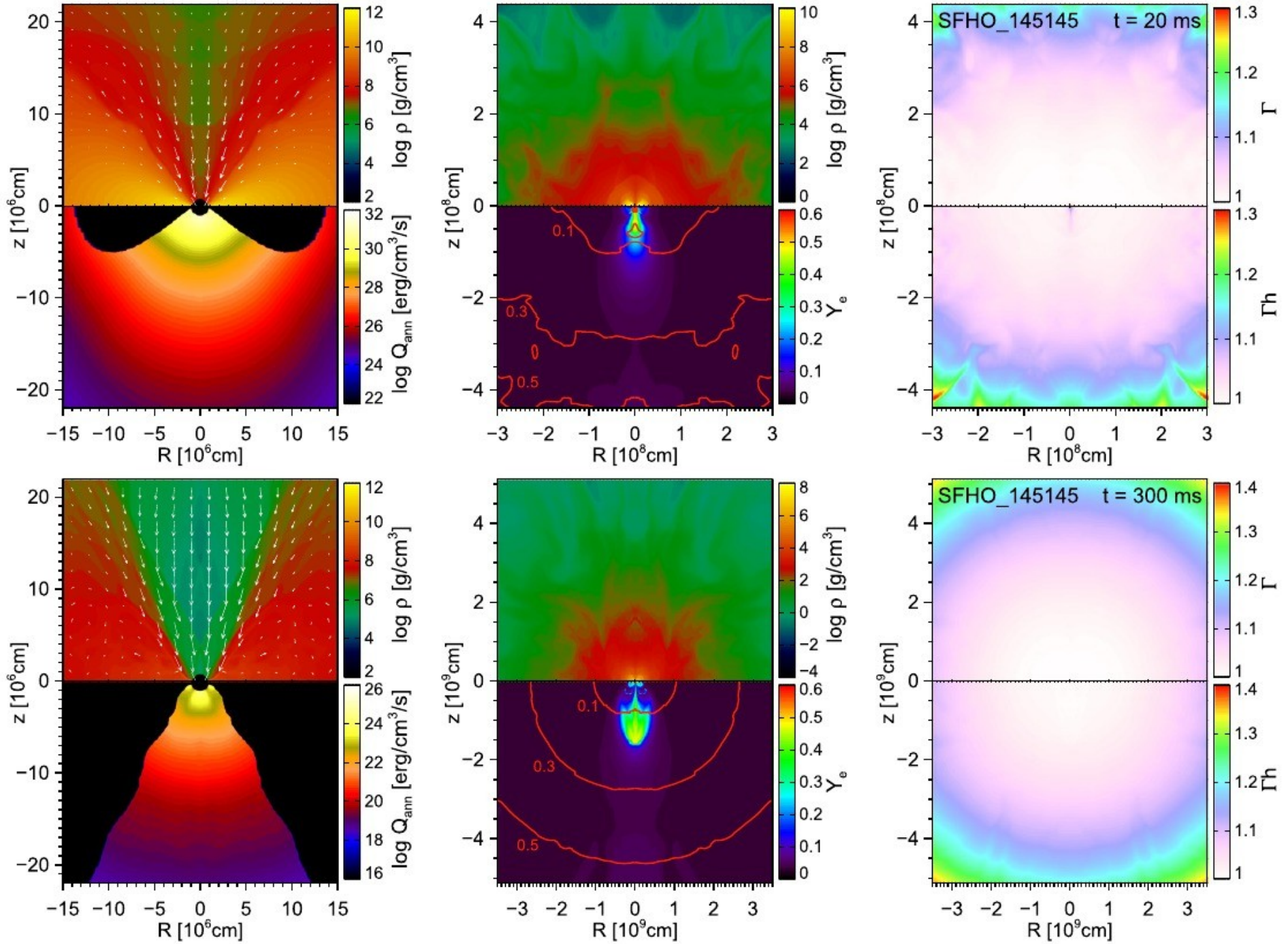

Figure 2. Maps of density, ρ, annihilation rate, $Q_{\rm ann}$, electron fraction, Y_e, Lorentz factor, Γ, and terminal Lorentz factor, Γh, for NS–NS merger model SFHO_145145 at the two times indicated in the right panel of each row. Note the different spatial and color scales for different times. Arrows indicate the poloidal (i.e., projected into the R–z plane) velocity vectors. Their length is limited to the distance between two neighboring arrows, which corresponds to 0.2 c. The red lines are isocontours of the poloidal velocity at values labeled in units of c.

Just et al., ApJL 816 (2016) 30

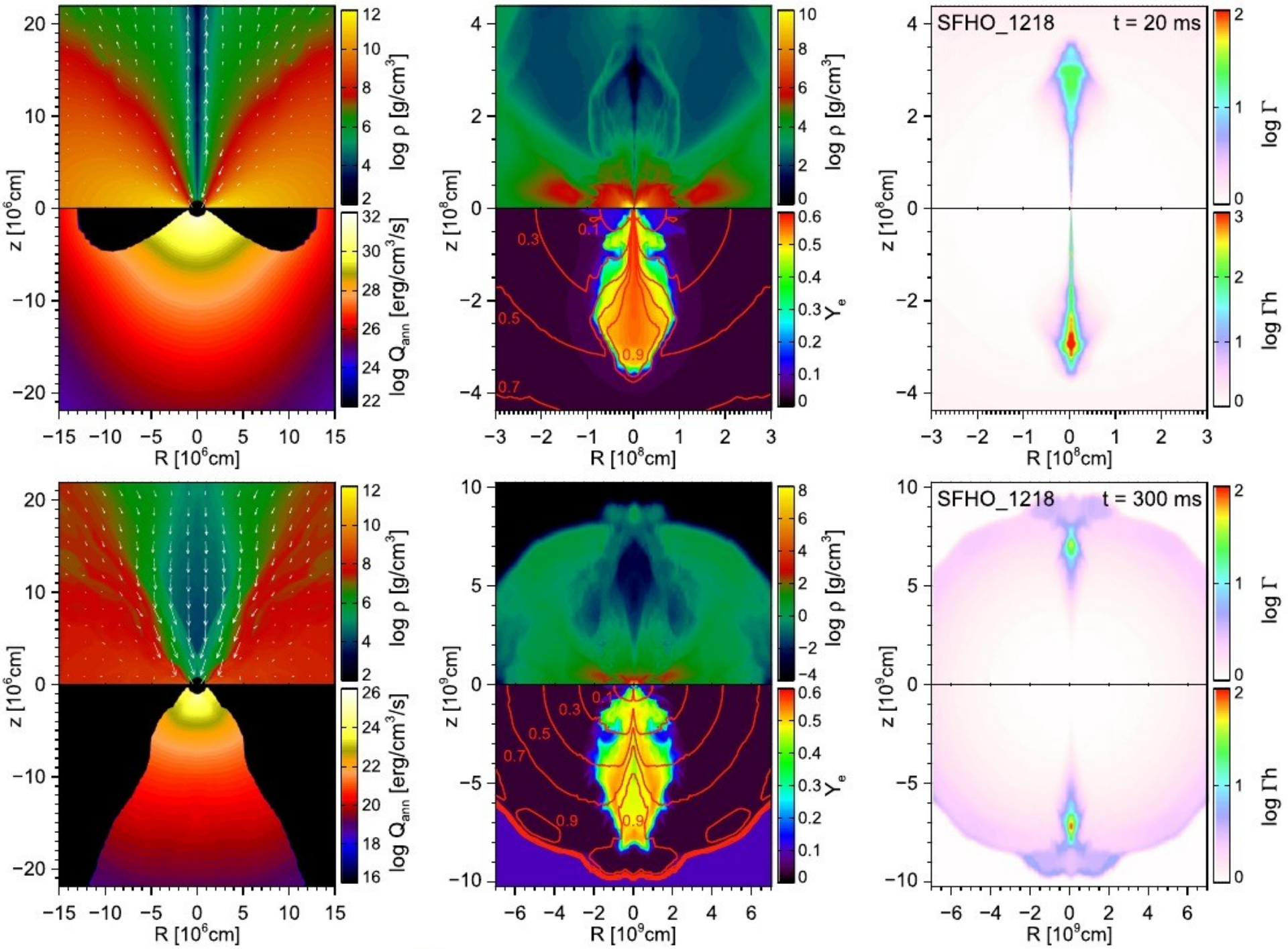

Figure 3. Same as Figure 2, but for model SFHO_1218 and with partially different spatial and color scales.

Just et al., ApJL 816 (2016) 30

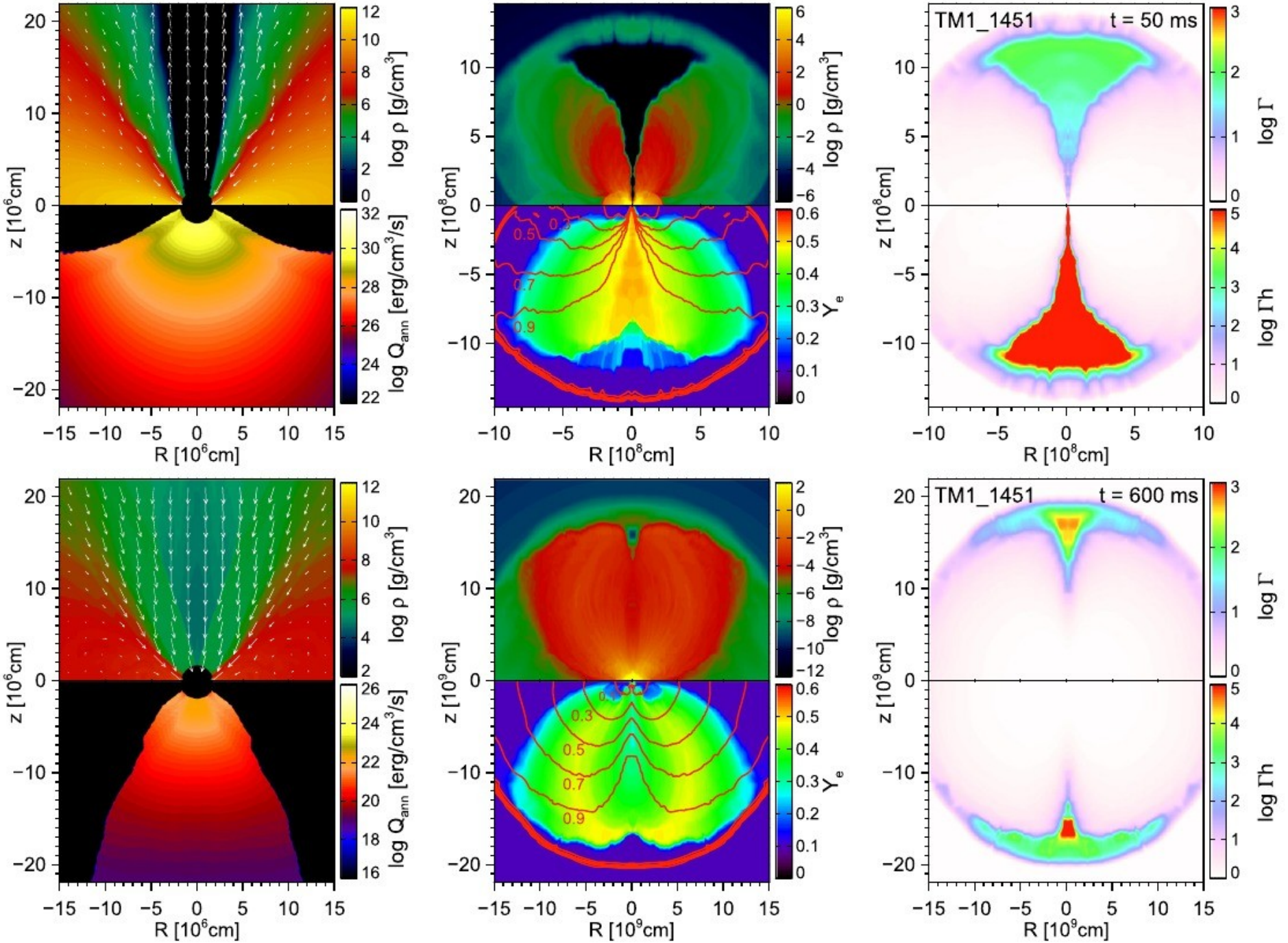

Figure 4. Same as Figure 2, but for NS–BH merger model TM1_1451 and with partially different spatial and color scales.

Extreme Magnetic Field Amplification

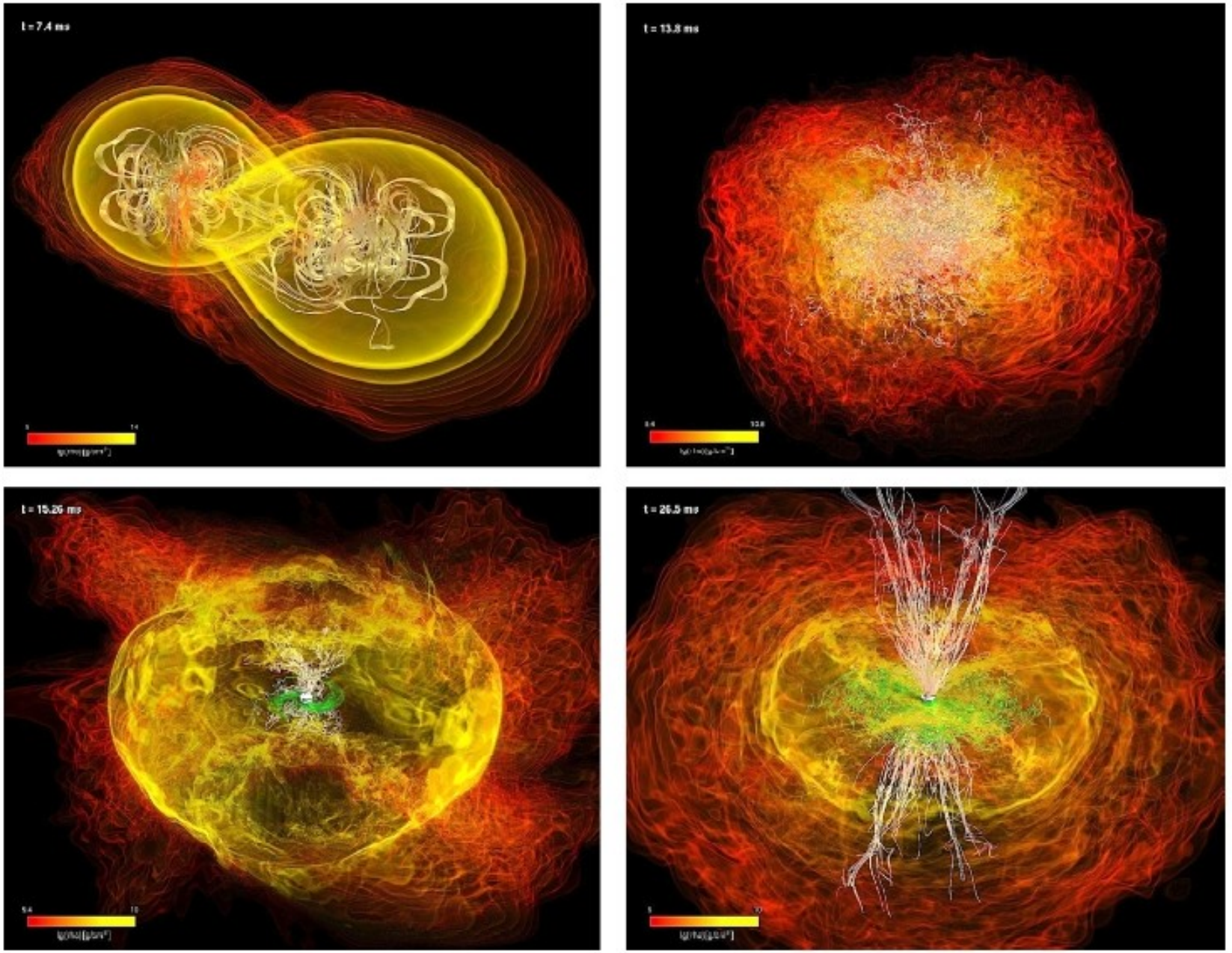

Rezzolla, Giacomazzo, Baiotti, et al., ApJL (2011)

Can the Extreme Magnetic Fields Power Jet Outflows?

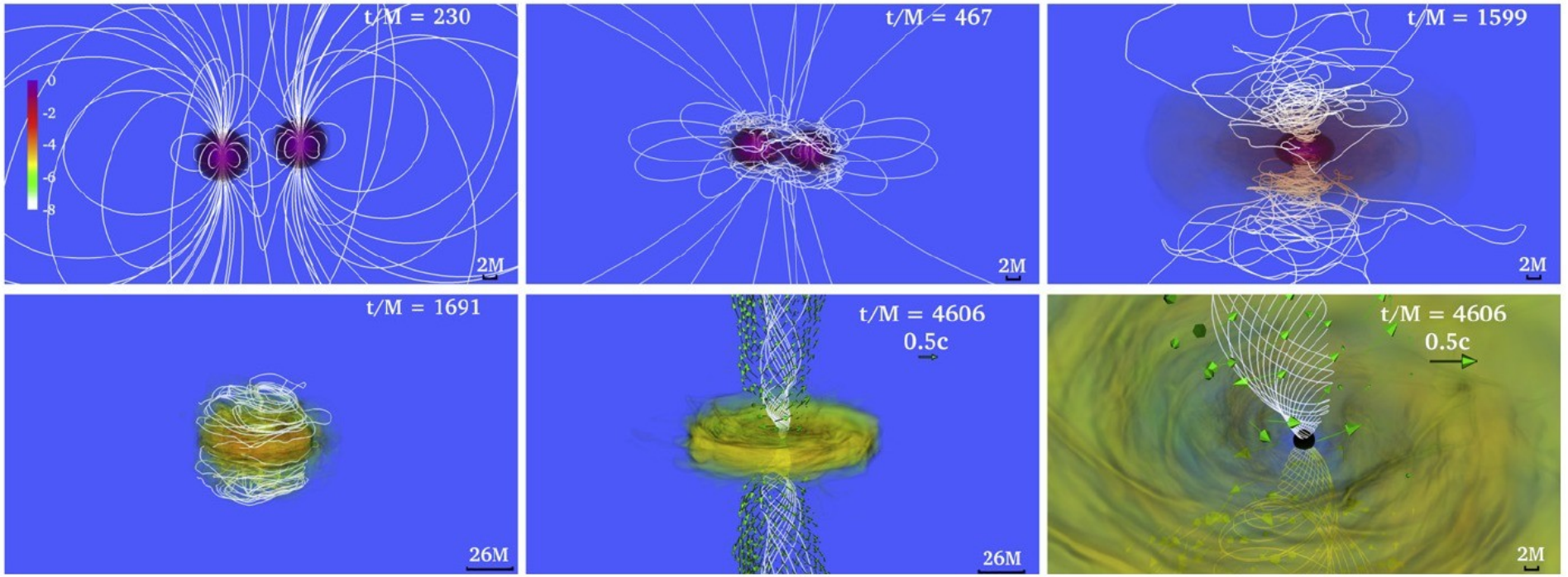

Figure 1. Snapshots of the rest-mass density, normalized to its initial maximum value $\rho_{0,\max} = 5.9 \times 10^{14}\,(1.625\,M_\odot/M_{\rm NS})^2$ g cm^{-3} (log scale) at selected times for the P case. The arrows indicate plasma velocities, and the white lines show the B-field structure. The bottom middle and right panels highlight the system after an incipient jet is launched. Here $M = 1.47 \times 10^{-2}(M_{\rm NS}/1.625\,M_\odot)$ ms $= 4.43\,(M_{\rm NS}/1.625\,M_\odot)$ km.

Ruiz, Lang, Paschalidis, & Shapiro, ApJL 824 (2016) L6

Mass Ejection From Compact Binary Mergers

Outflows from Compact Binary Mergers

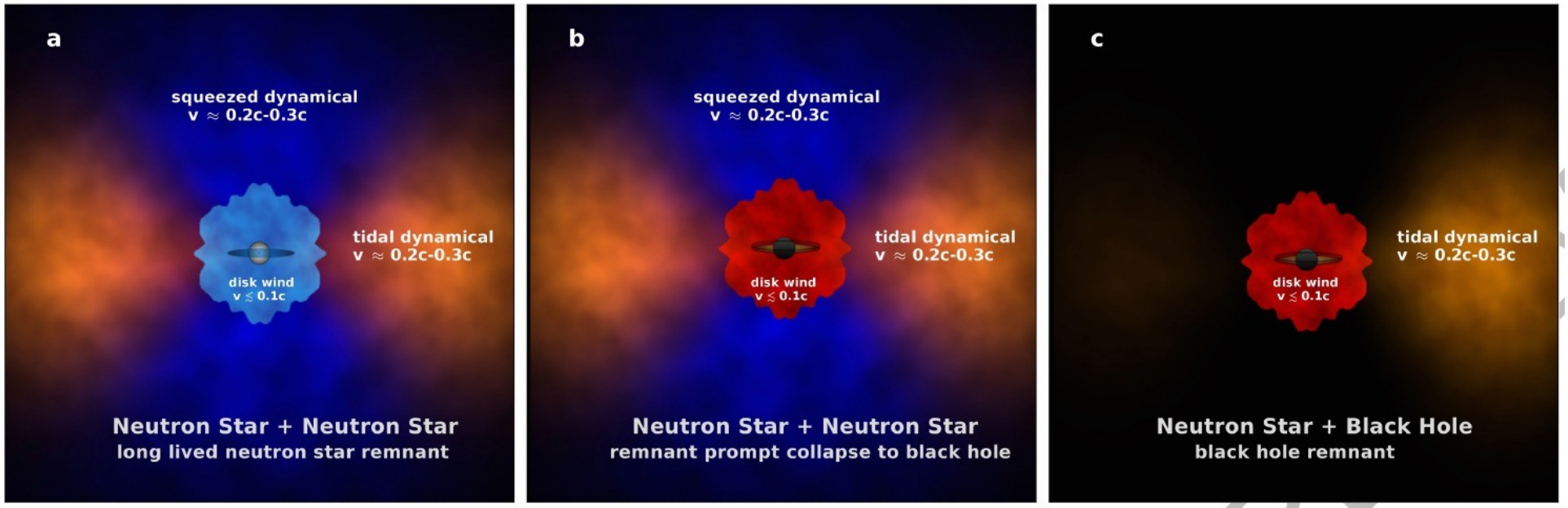

Figure 1 | Schematic illustration of the components of matter ejected from neutron star mergers. Red colours denote regions of heavy r-process elements, which radiate red/infrared light. Blue colours denote regions of light r-process elements which radiate blue/optical light. During the merger, tidal forces peel off tails of matter, forming a torus of heavy r-process ejecta in the plane of the binary. Material squeezed into the polar regions during the stellar collision can form a cone of light r-process material. Roughly spherical winds from a remnant accretion disk can also contribute, and are sensitive to the fate of the central merger remnant. **a**, If the remnant survives as a hot NS for tens of milliseconds, its neutrino irradiation lowers the neutron fraction and produce a blue wind. **b**, If the remnant collapses promptly to a black hole, neutrino irradiation is suppressed and the winds may be red. **c**, In the merger of NS and a black hole, only a single tidal tail is ejected and the disk winds are more likely to be red.

(Kasen, Metzger et al., Nature 2017)

Spiral Arms in Newtonian Simulations

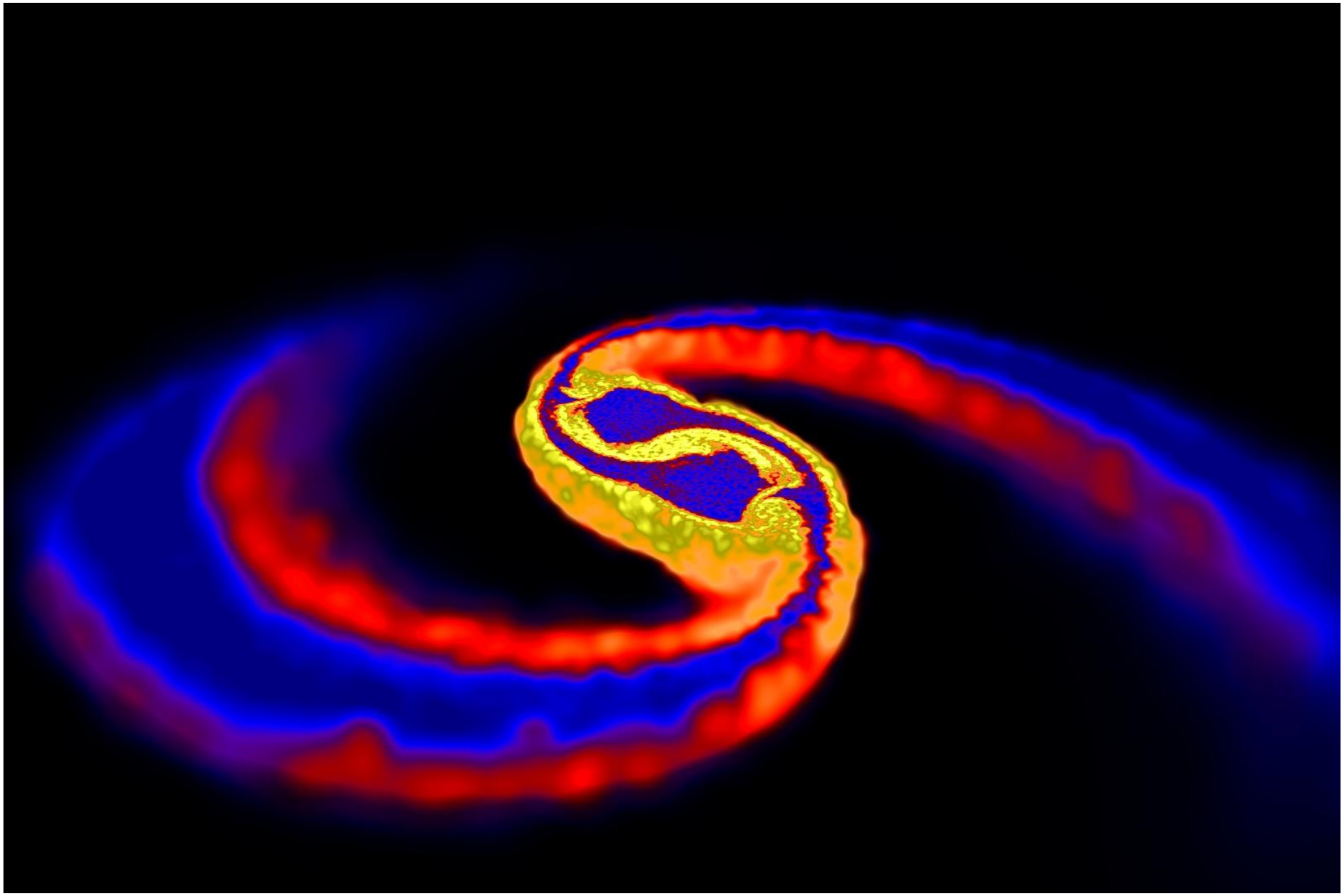

(Courtesy: S. Rosswog)

Dynamical Mass Ejection in Relativistic Simulations

Symmetric NS-NS merger

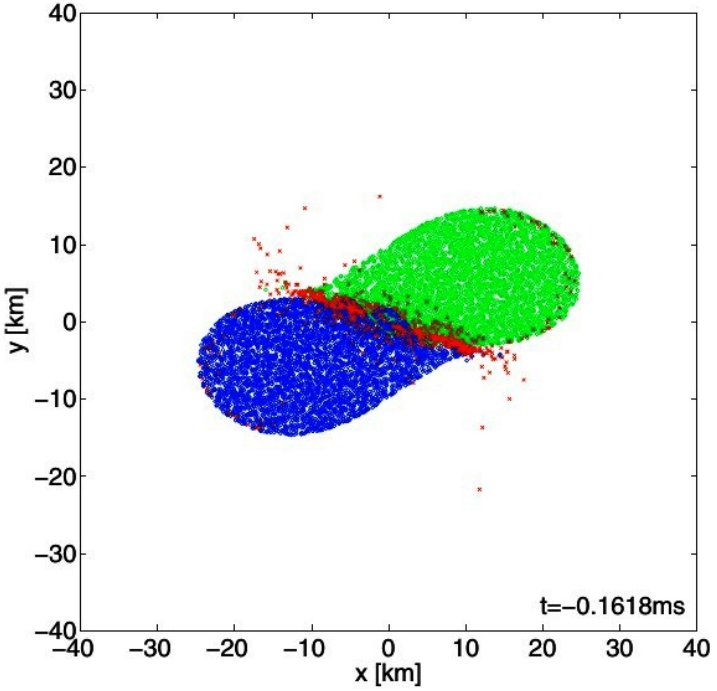

Asymmetric NS-NS merger

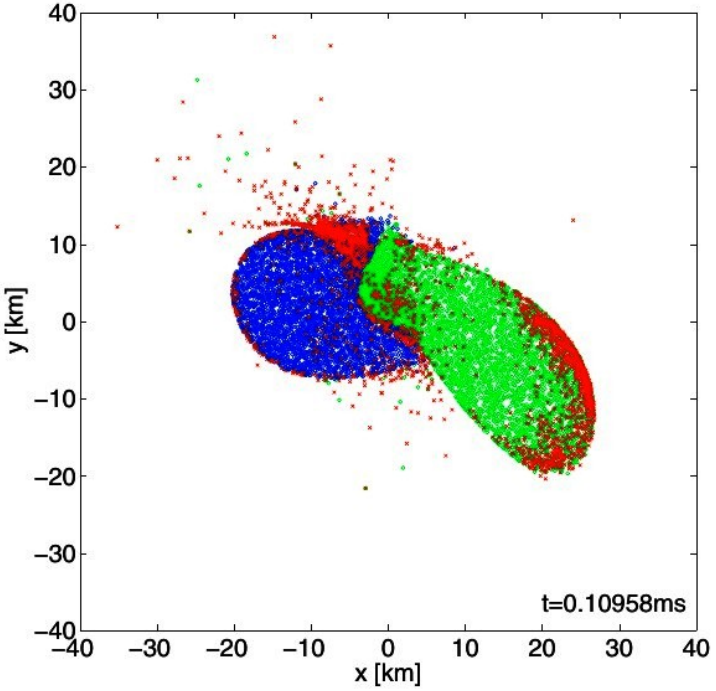

Fig. 14. Snapshots at the moment of merging of a symmetric (S1414; *left*) and an asymmetric (S1216; *right*) model. The particles color-coded in red become gravitationally unbound during the postmerger evolution. We can identify two sources of ejected matter, the merger interface and the tip of the primary spiral arm (if present). Note that the ejected matter is over-emphasized in this plot since we plotted every second ejecta particle whereas for the remaining matter only every 10th particle near the equatorial plane is plotted. The red particles at the contact interface are therefore squeezed out perpendicular to the orbital plane.

(Oechslin, Janka, Marek; A&A 467 (2007) 395)

Dynamical Mass Ejection in Relativistic Simulations

Symmetric NS-NS merger

Asymmetric NS-NS merger

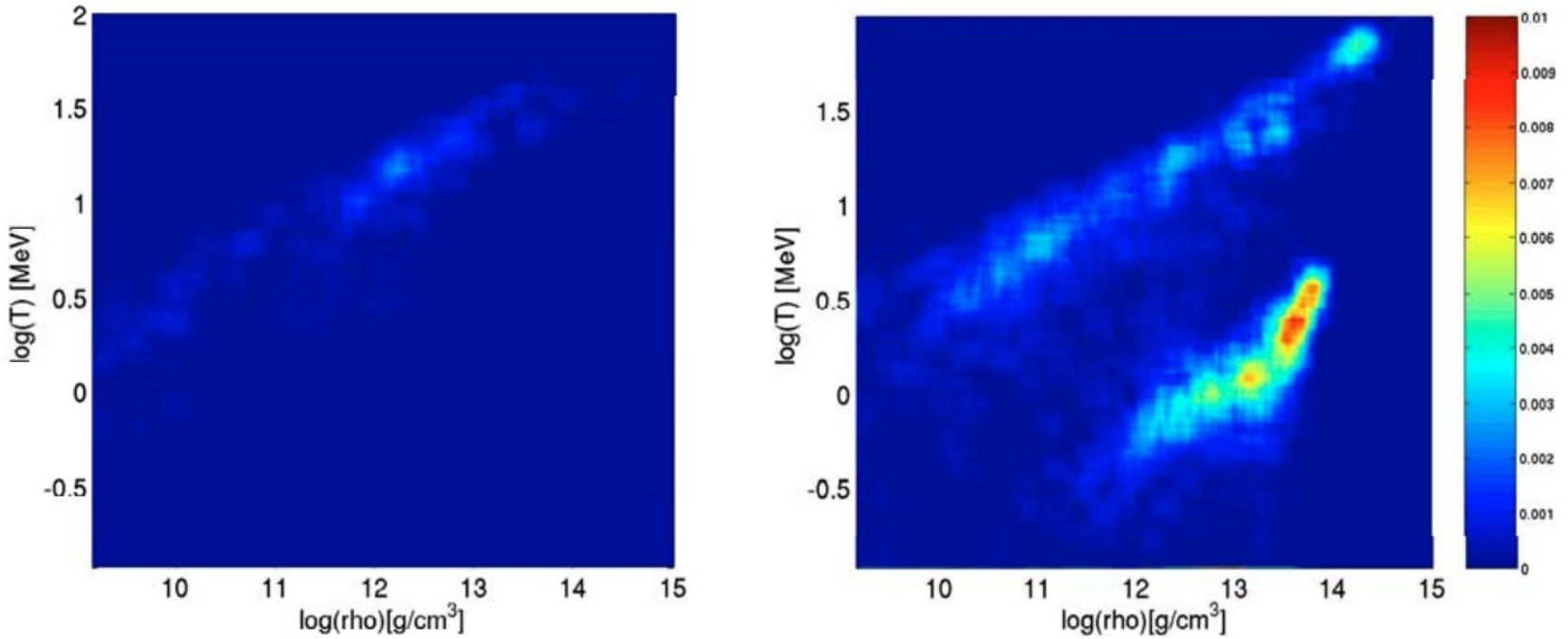

Fig. 15. Shown is the distribution of ejected matter in the density-temperature plane around 1 ms after merging for models S1414 (*left*) and S1216 (*right*). Color-coded is the amount of ejecta matter per unit of density and temperature. We can identify two contributions to the ejecta, a cold/low-entropy component and a hot/high-entropy one. The cold component is only present in model S1216, which suggests that this matter comes from the tip of the spiral arm, while the hot component that exists in both cases stems from the merger interface.

(Oechslin, Janka, Marek; A&A 467 (2007) 395)

Origin of Dynamically Ejected Mass

Symmetric NS-NS merger

Asymmetric NS-NS merger

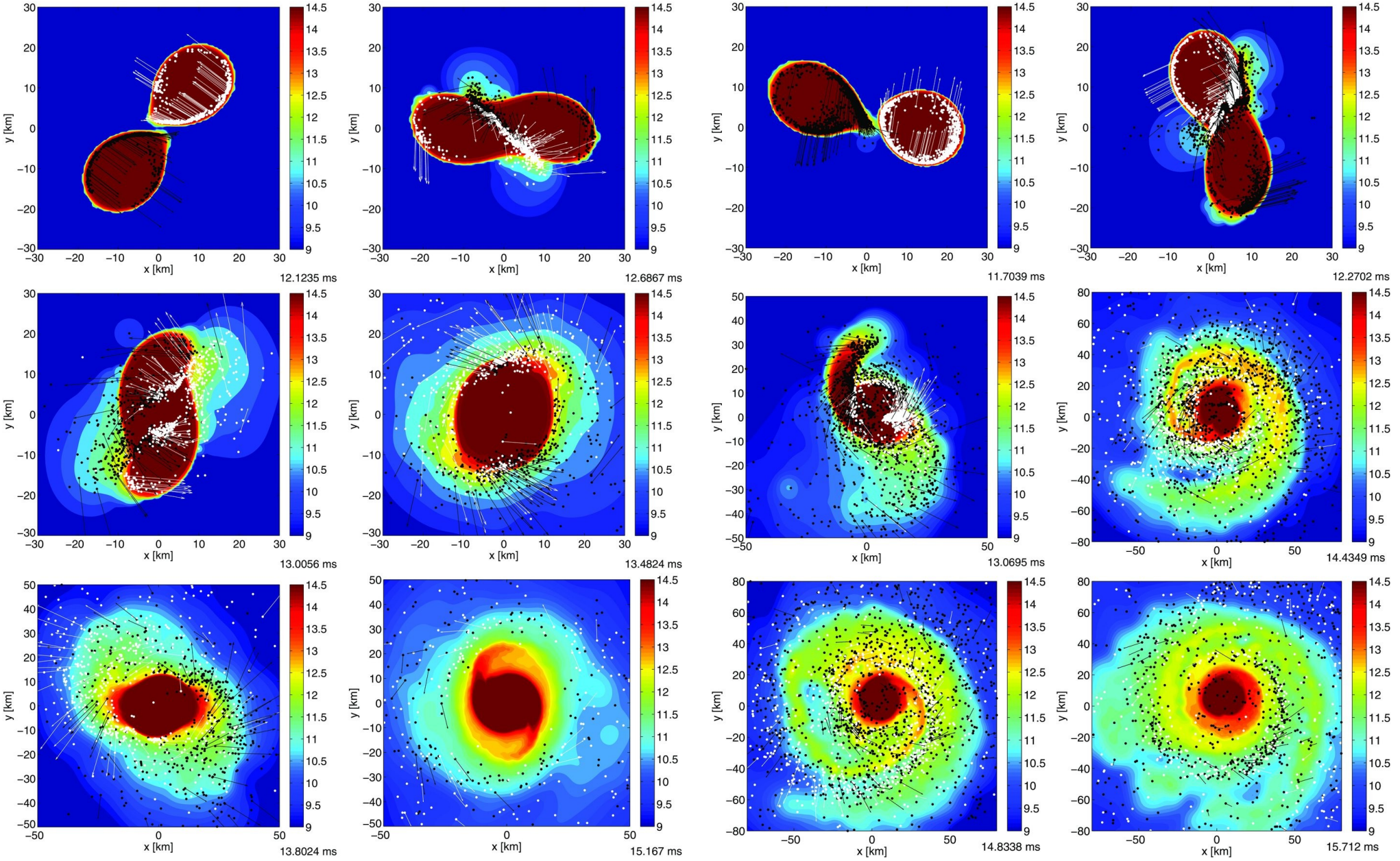

(Bauswein, Goriely, Janka, Marek; ApJ 773 (2013) 78)

Vertical Structure of Dynamical Ejecta

Symmetric NS-NS merger

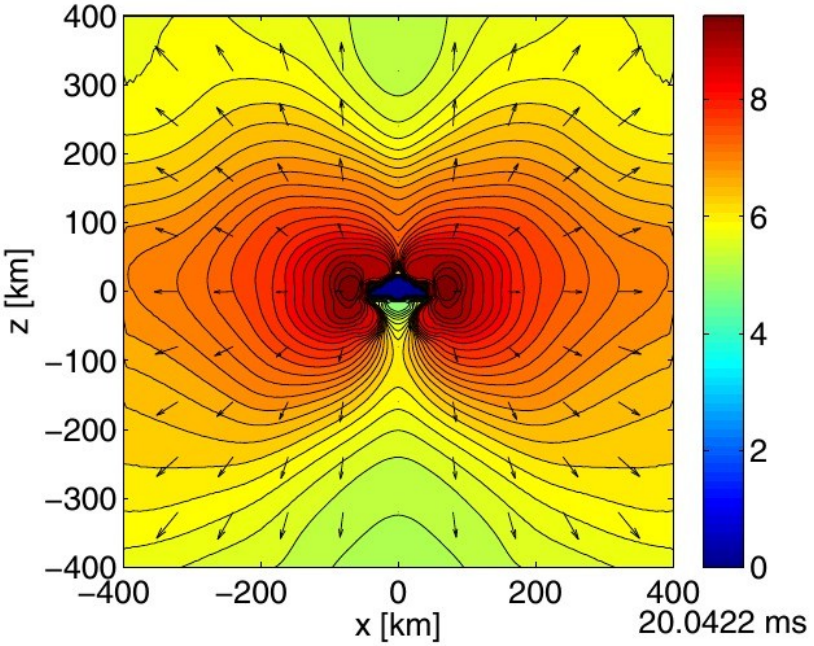

Asymmetric NS-NS merger

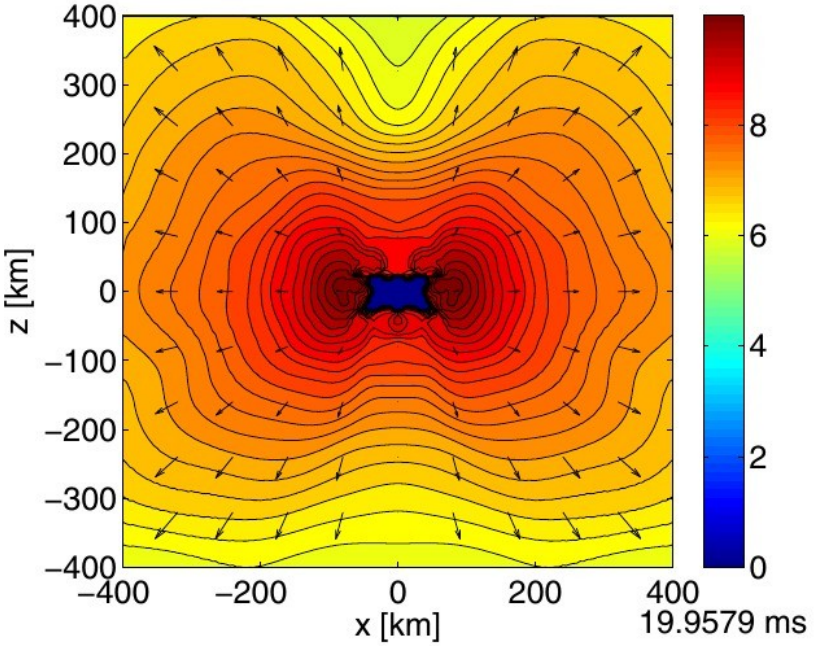

Figure 6. Ejecta geometry visualized by the rest-mass density (color-coded and logarithmically plotted in g cm^{-3}) excluding matter of the bound central remnant for the 1.35–1.35 $M_\odot$ merger (left) and the 1.2–1.5 $M_\odot$ merger (right) with the DD2 EOS. Density contours are obtained by azimuthal averaging. Arrows represent the coordinate velocity field where an arrow length of 200 km corresponds to the speed of light. The time of the snapshots is given below the color bar of each panel. The visualization tool SPLASH was used to convert SPH data to grid data (Price 2007).

(Bauswein, Goriely, Janka, Marek; ApJ 773 (2013) 78)

Dynamical Mass Ejection from Compact Binary Mergers

Symmetric NS-NS merger

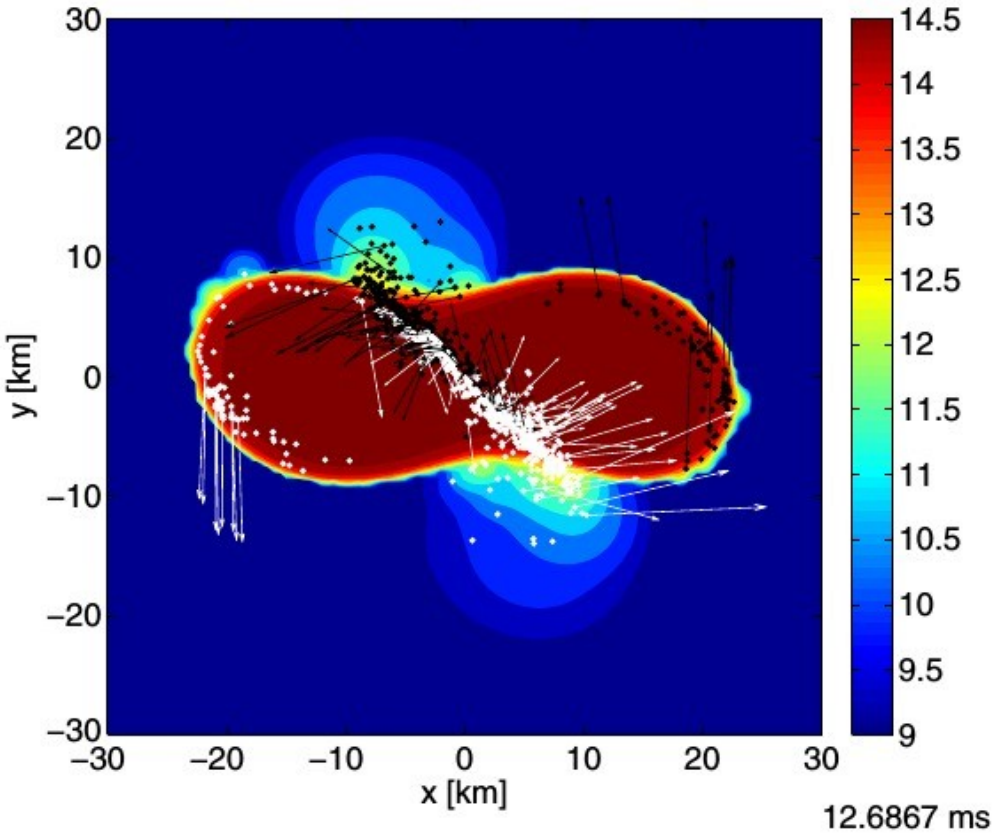

(Bauswein, Goriely, THJ, ApJ 773 (2013) 78)

NS-BH merger

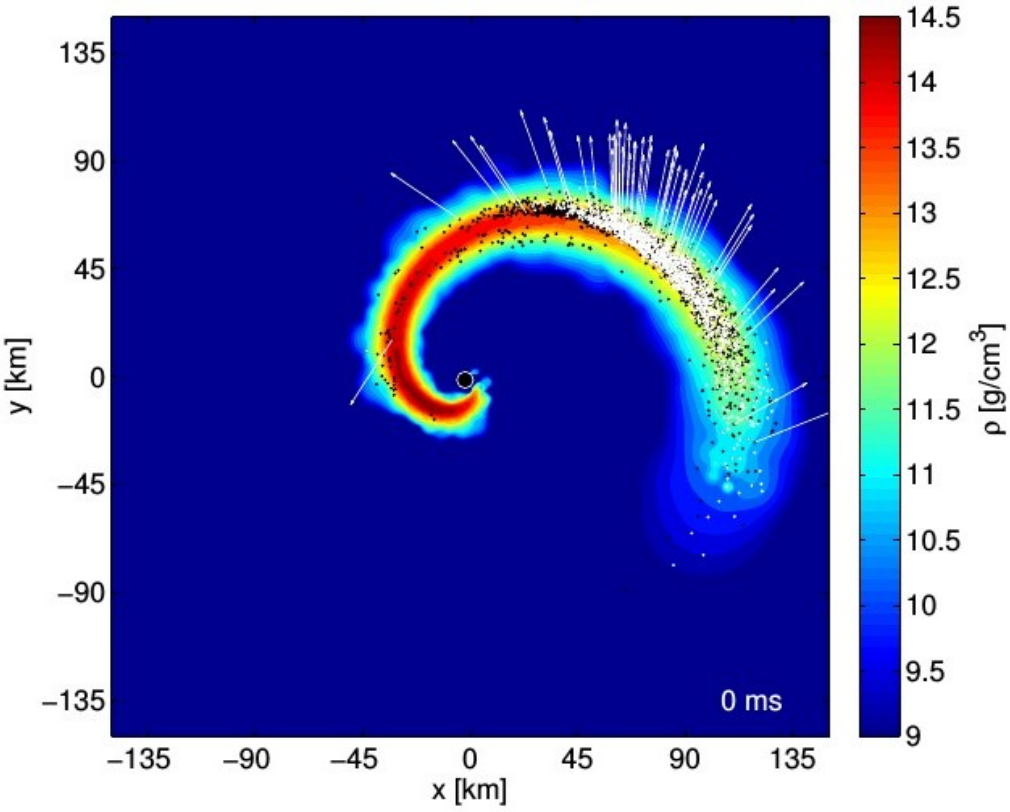

(Just et al., MNRAS 448 (2015) 541)

Systematics of Dynamical Mass Ejection from Binary Neutron-Star Mergers

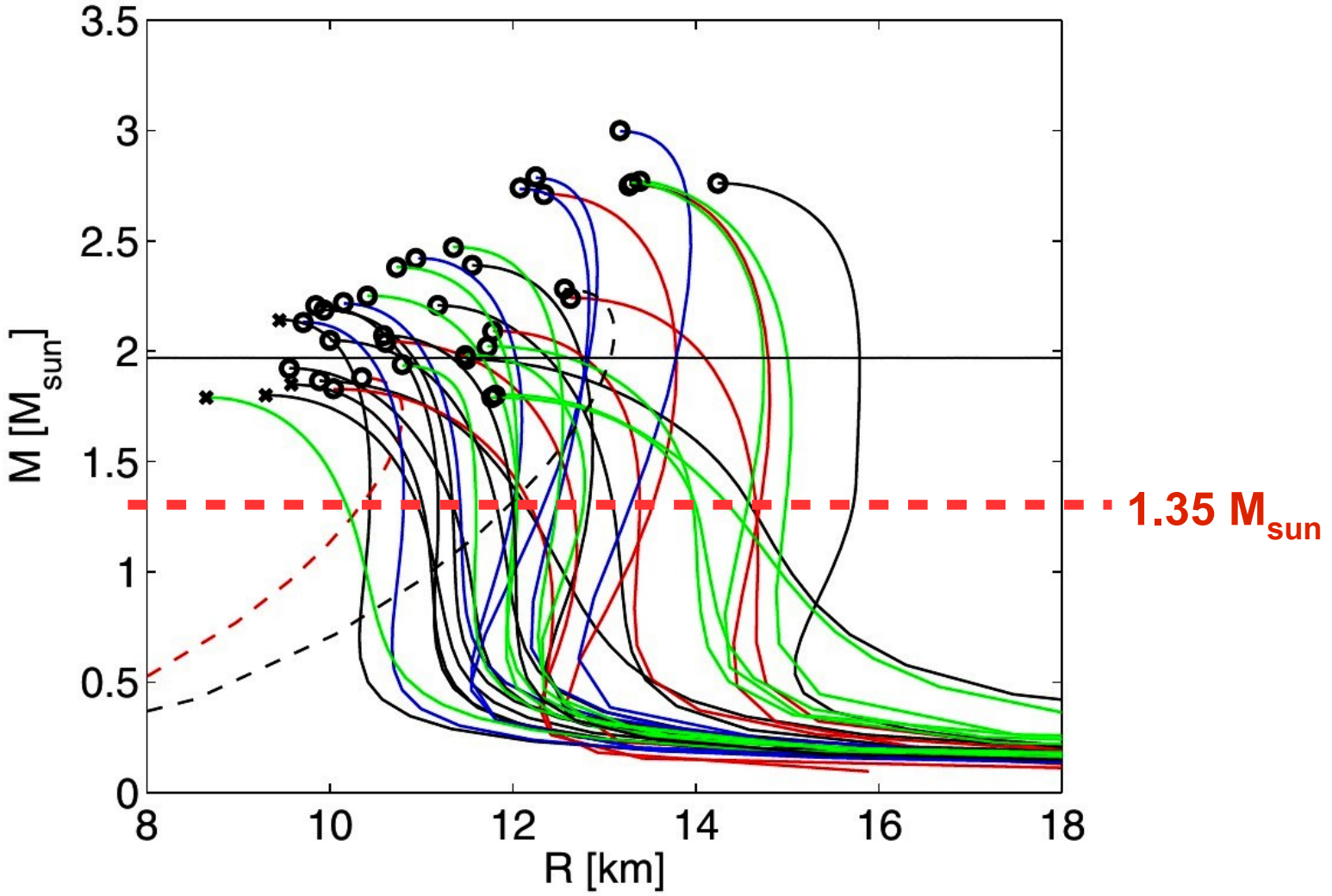

(Bauswein, Janka, Hebeler, Schwenk, PRD 86 (2012) 063001)

Systematics of Dynamical Mass Ejection from Binary Neutron-Star Mergers

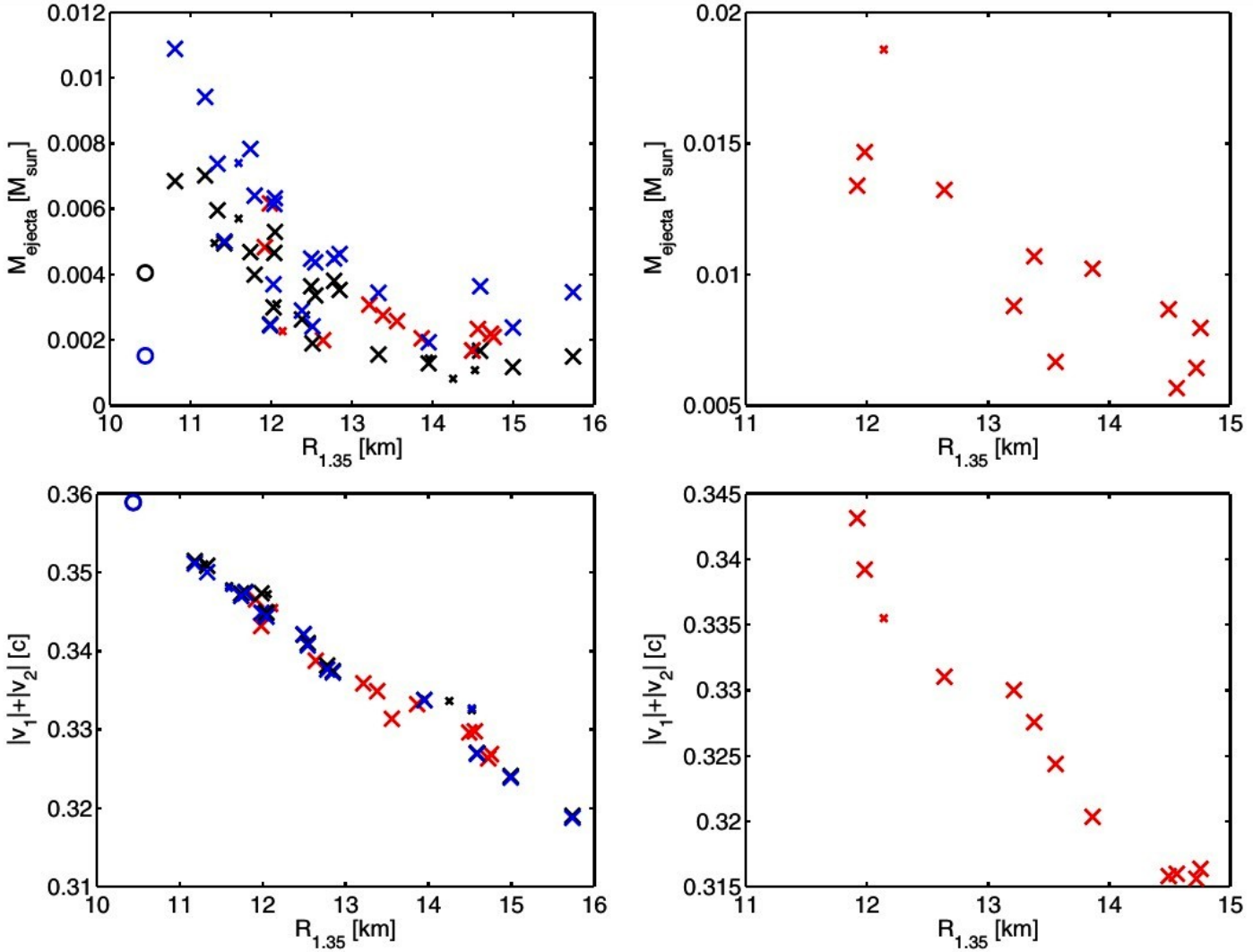

Figure 3. Amount of unbound material for 1.35–1.35 $M_\odot$ mergers (top left) and 1.2–1.5 $M_\odot$ mergers (top right) for different EOSs characterized by the corresponding radius $R_{1.35}$ of a nonrotating NS. Red crosses denote EOSs which include thermal effects consistently, while black (blue) symbols indicate zero-temperature EOSs that are supplemented by a thermal ideal-gas component with $\Gamma_{th} = 2$ ($\Gamma_{th} = 1.5$) (see main text). Small symbols represent EOSs which are incompatible with current NS mass measurements (Demorest et al. 2010; Antoniadis et al. 2013). Circles display EOSs which lead to the prompt collapse to a black hole. The lower panels display the sum of the maxima of the coordinate velocities of the mass centers of the two binary components as a function of $R_{1.35}$ for symmetric (bottom left) and asymmetric (bottom right) binaries.

(Bauswein, Goriely, Janka, Marek; ApJ 773 (2013) 78)

Systematics of Dynamical Mass Ejection from Binary Neutron-Star Mergers

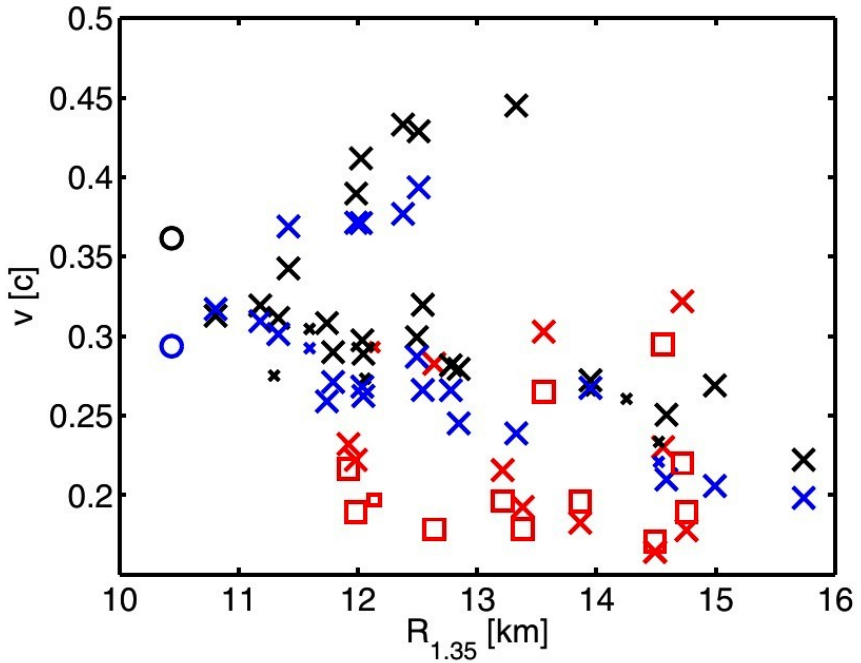

Figure 12. Average ejecta expansion velocity for 1.35–1.35 $M_\odot$ mergers (with symbols analogous to Figure 3) and for 1.2–1.5 $M_\odot$ (red squares) for different EOSs characterized by the corresponding radius $R_{1.35}$ of a nonrotating NS with a mass of 1.35 $M_\odot$.

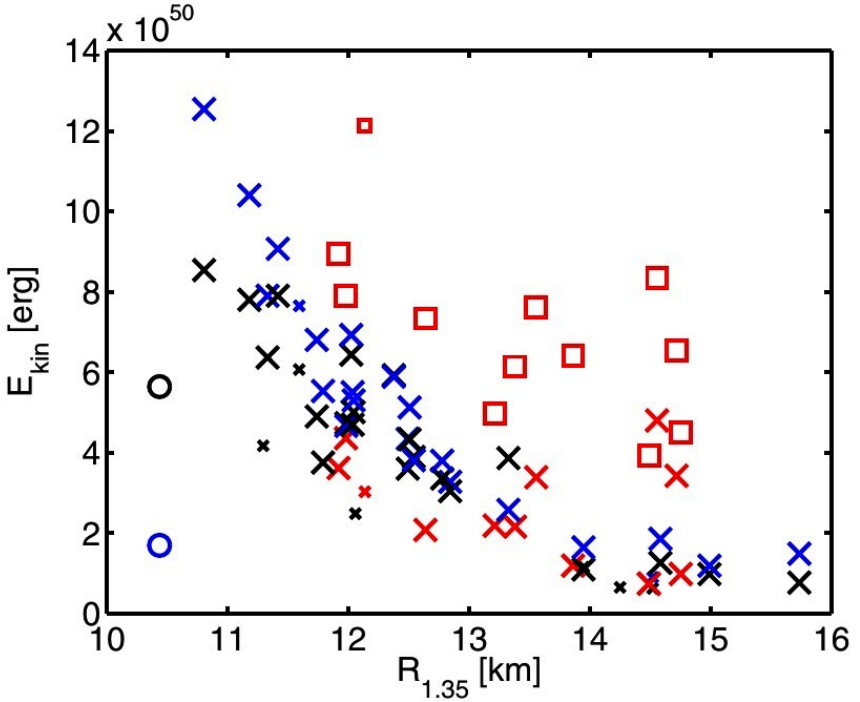

Figure 13. Kinetic energy of the ejecta for 1.35–1.35 $M_\odot$ mergers (with symbols analogous to Figure 3) and for 1.2–1.5 $M_\odot$ (red squares) for different EOSs characterized by the corresponding radius $R_{1.35}$ of a nonrotating NS with a mass of 1.35 $M_\odot$.

(Bauswein, Goriely, Janka, Marek; ApJ 773 (2013) 78)

Nucleosynthesis in Dynamical Merger Ejecta

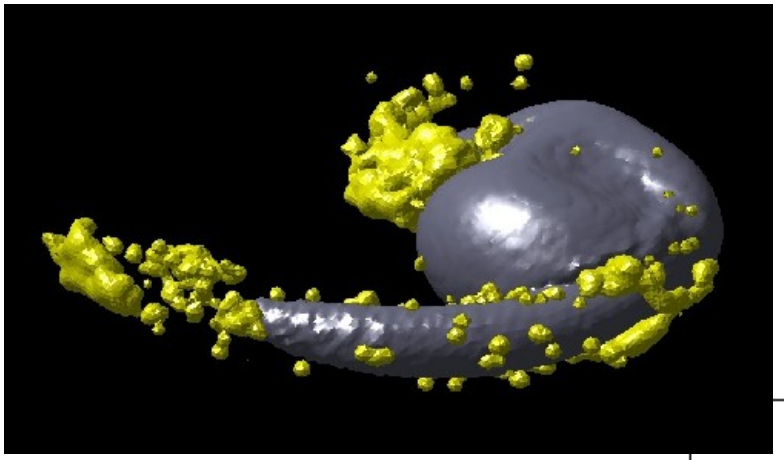

(Goriely, Bauswein, THJ, ApJL 738 (2011) L32)

During r-processing fission recycling takes place and produces roughly solar abundances for A > 130.

Per merger event 10^{-3}–10^{-2} M_{sun} are ejected.

With rate of 10^{-5} events per year and galaxy, NS mergers could be the main source of heavy r-process material.

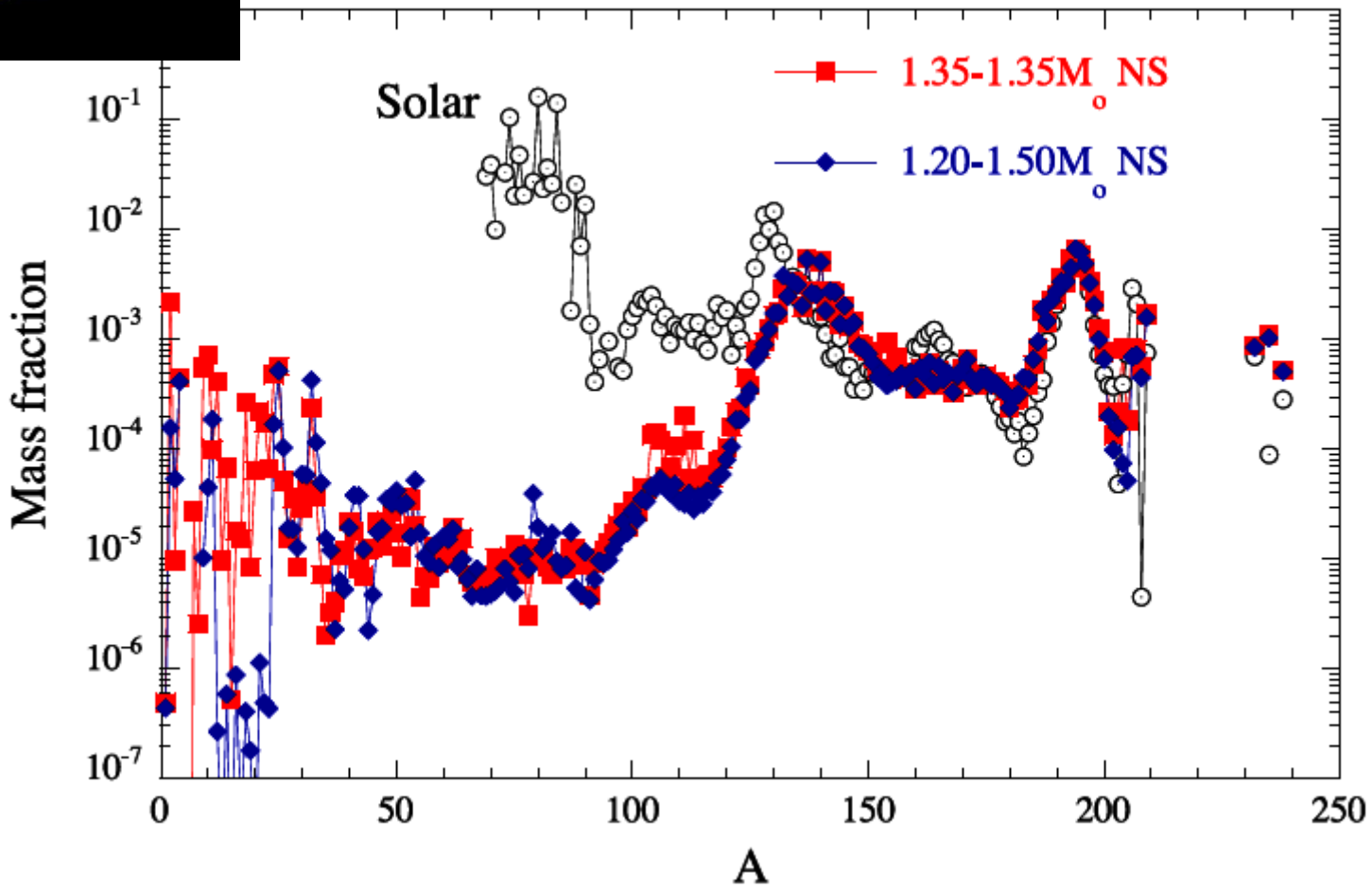

Nucleosynthesis in Neutrino-processed Merger Ejecta

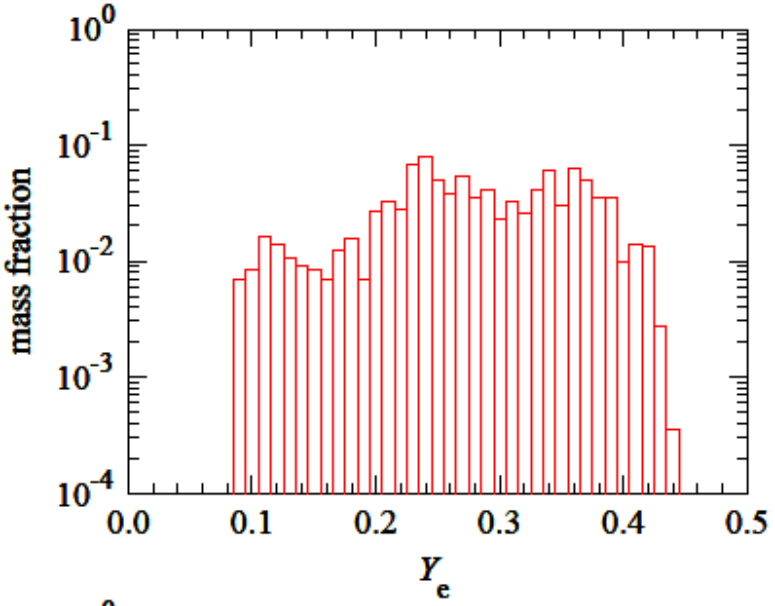

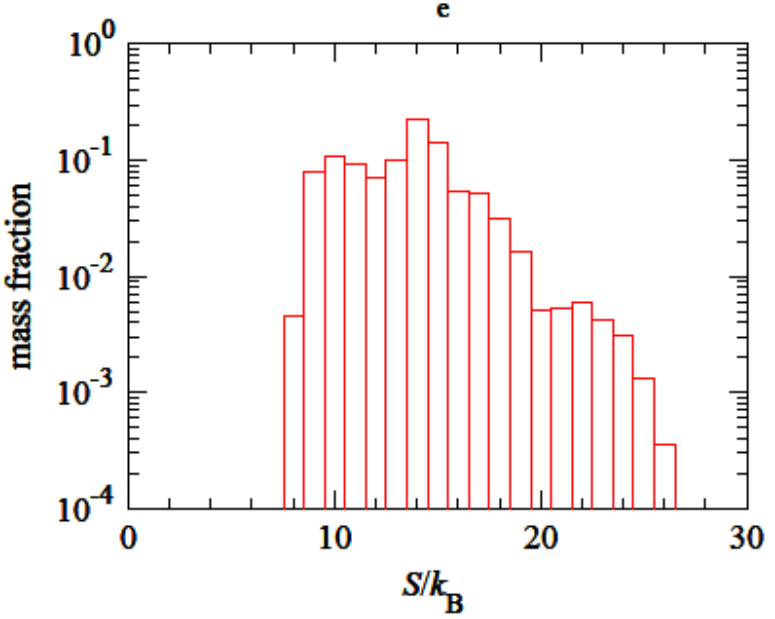

(Wanajo et al., ApJL 789 (2014) L39)

- Compact NSs produce strongly shock-heated ejecta.
- Electron fraction increases considerably in hot ejecta, mostly due to positron capture.
- Heavy r-process is still produced, but also A < 130 nuclei.

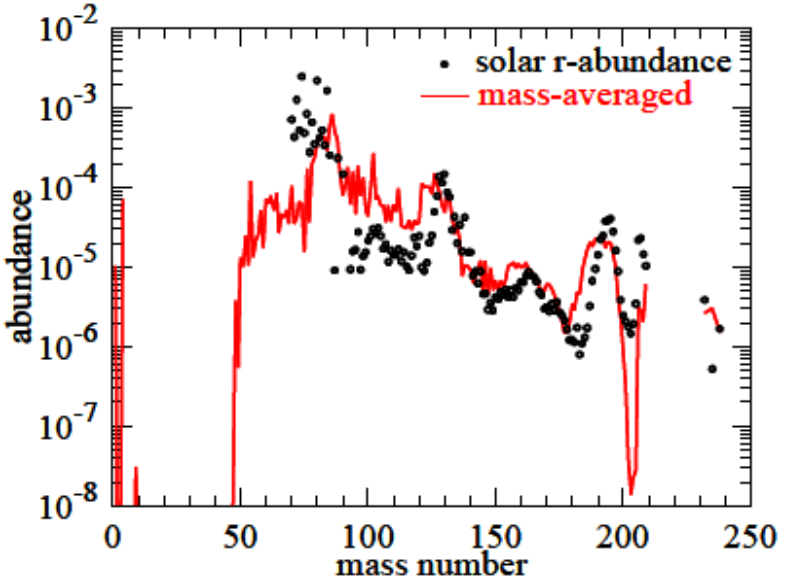

BH-torus Outflows

- Hydrodynamical 2D models of BH-torus evolution.
  (Just, PhD Thesis 2012)
- New Newtonian MHD-code with 2D, energy-dependent neutrino transport based on two-moment closure scheme.
  (Obergaulinger, PhD Thesis 2008)
- BH treated by Artemova-Novikov potential.
- Diplayed model based on Shakura-Sunyaev α-viscosity
- MHD yields turbulent tori !

Just et al., MNRAS 448 (2015) 541

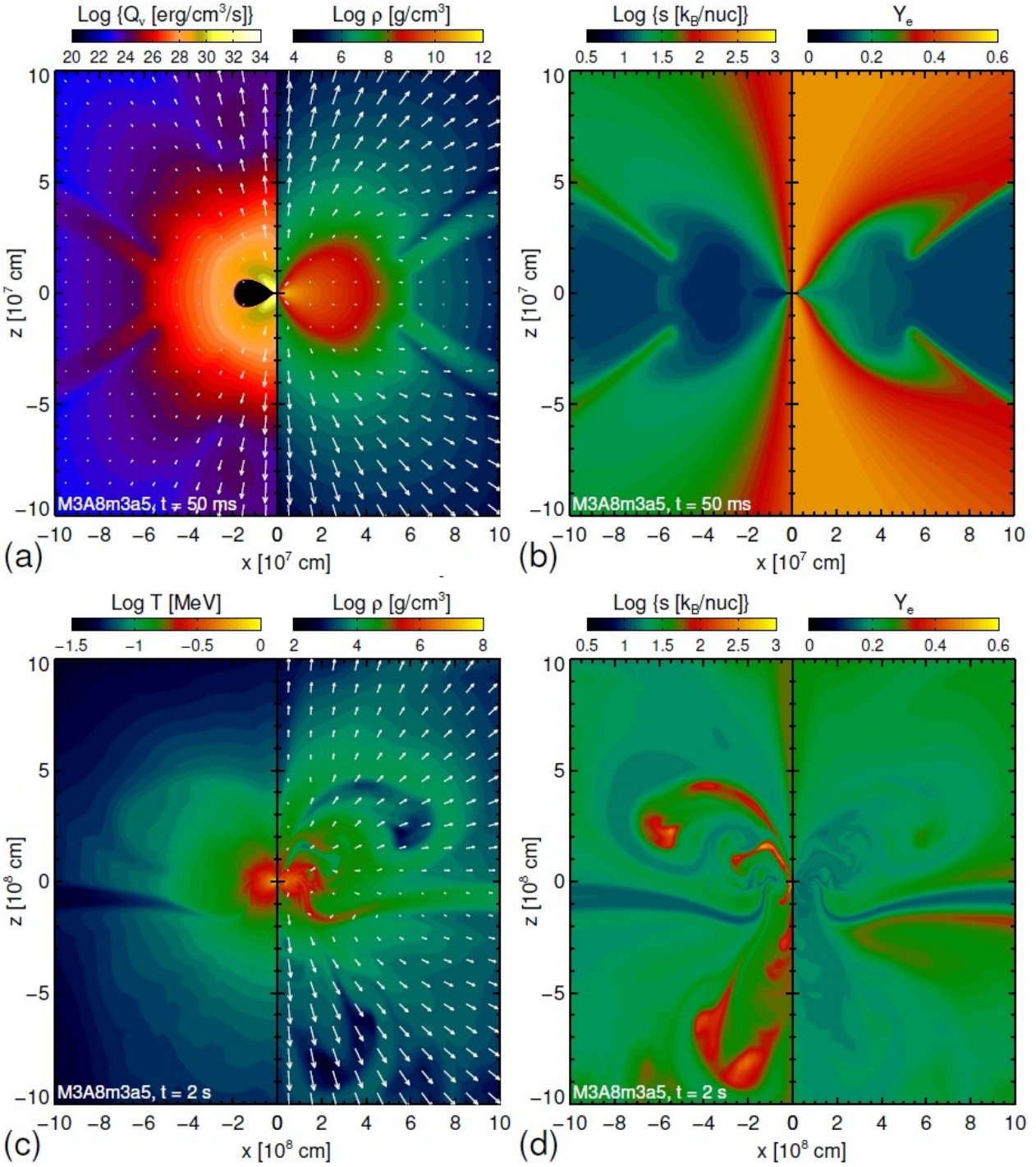

For BH-disk ejecta, see also Fernández & Metzger (2014), Wu+ (2016); Siegert & Metzger (2017); for HMNS winds, see Perego+ (2014), Fernández+ (2015), Martin+ (2015), Fujibayashi+ (2017)

r-process Nucleosynthesis

Ejecta from NS+NS merger + BH-torus remnant

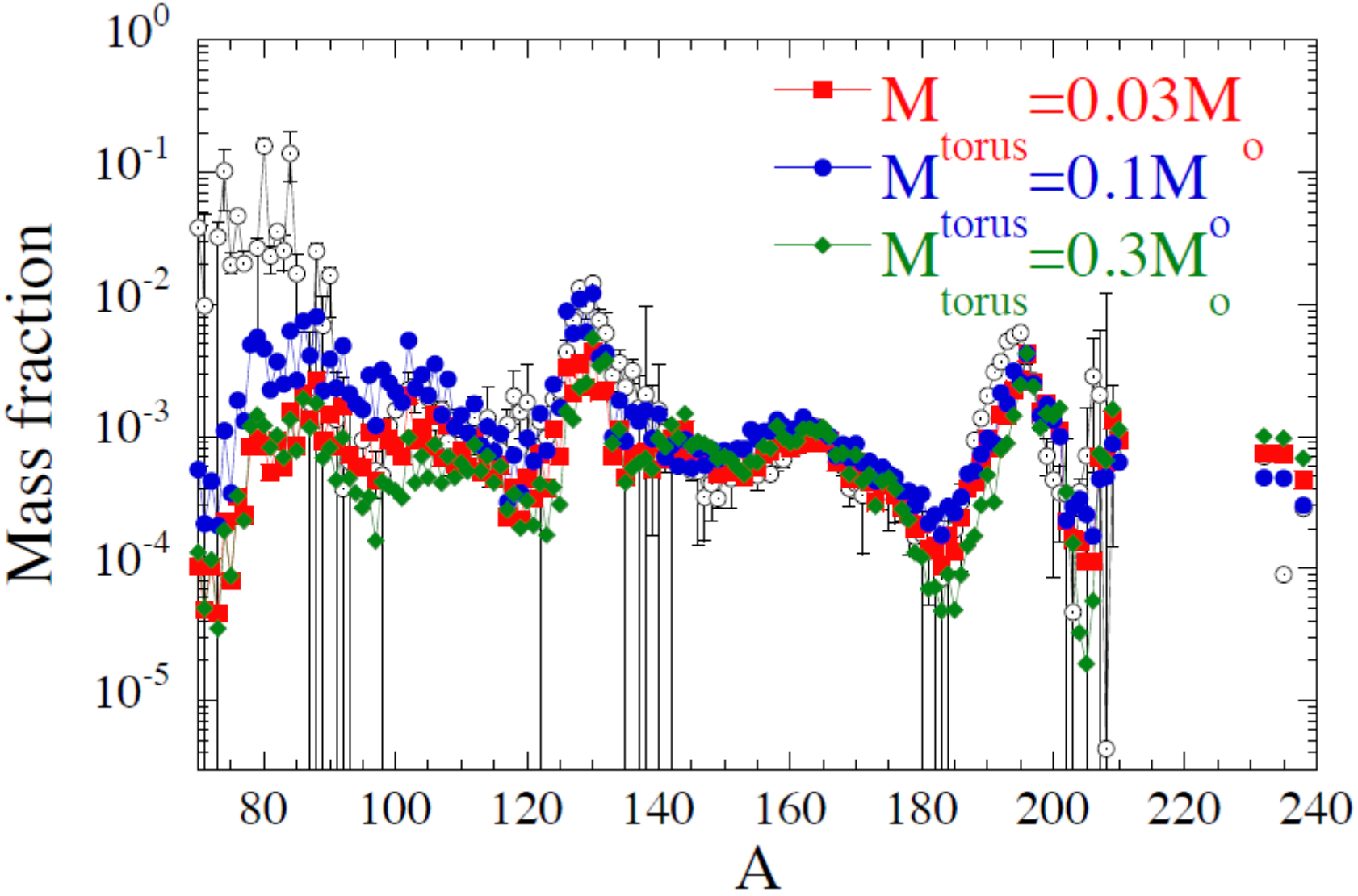

(Just et al, MNRAS 448 (2015) 541)

For BH-disk ejecta, see also Fernández & Metzger (2014), Wu+ (2016); Siegert & Metzger (2017);
for HMNS winds, see Perego+ (2014), Fernández+ (2015), Martin+ (2015), Fujibayashi+ (2017)

Outflows from Magnetized BH-torus

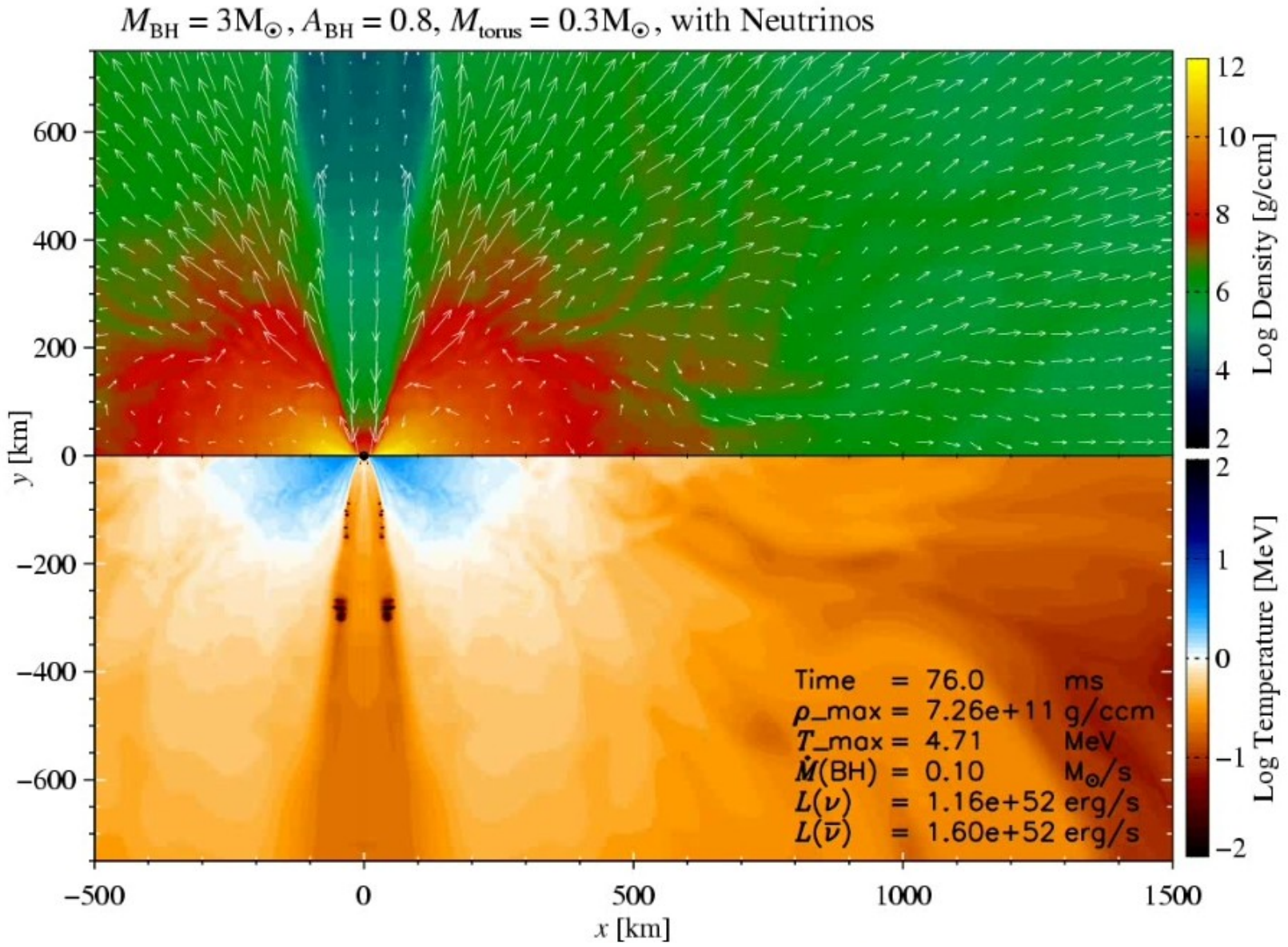

Magnetohydrodynamic simulation
With M1 ALCAR neutrino transport

(Just, PhD Thesis 2012)

Improved Leakage-Equilibration-Absorption Scheme (ILEAS)

Leakage

- Effective local neutrino loss rates
- Interpolation: diffusion - free streaming
- Three species: ν_e , $\bar{\nu}_e$, ν_x

Equilibration

- Lepton fraction advection
- Neutrino β-equilibrium EoS
- Equilibration step

Absorption

- Neutrino absorption rates
- Ray tracing

R. Ardevol-Pulpillo, PhD Thesis; Ardevol-Pulpillo, Janka, Just & Bauswein (in preparation)

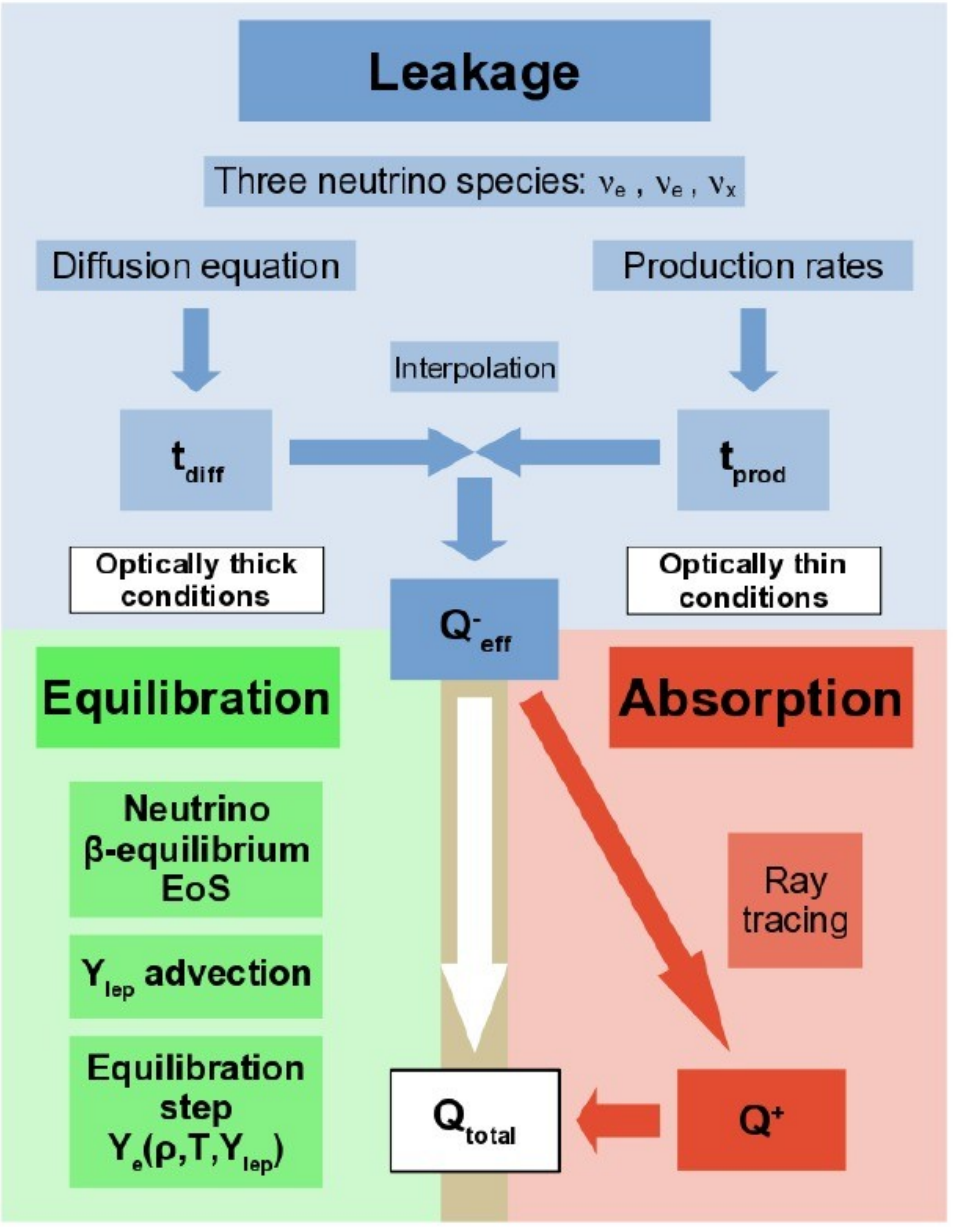

Improved Leakage-Equilibration-Absorption Scheme (ILEAS)

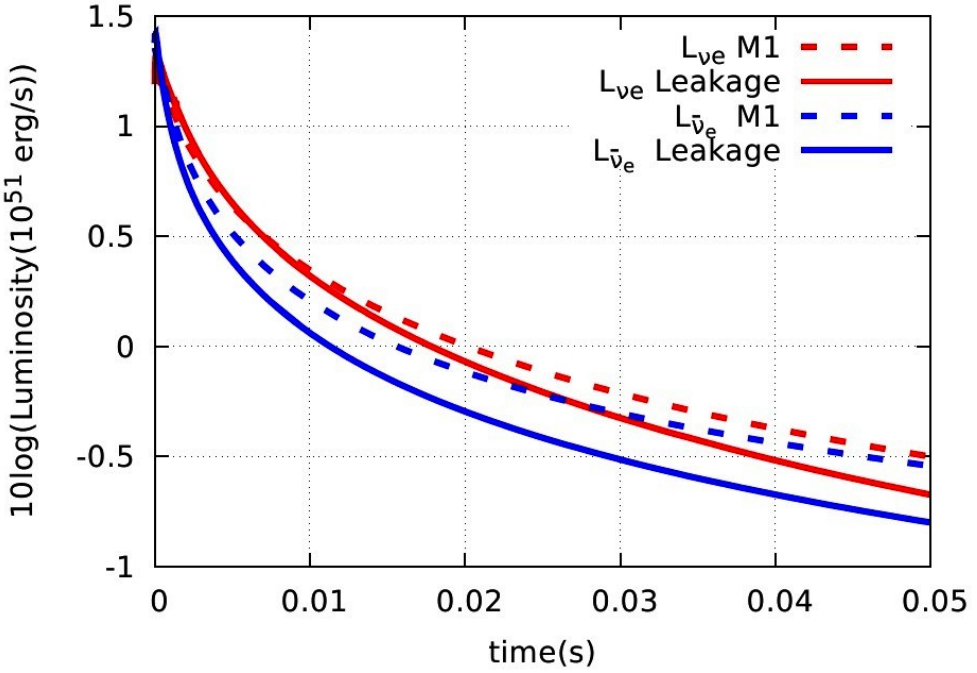

R. Ardevol-Pulpillo, PhD Thesis; Ardevol-Pulpillo, Janka, Just & Bauswein (in preparation)

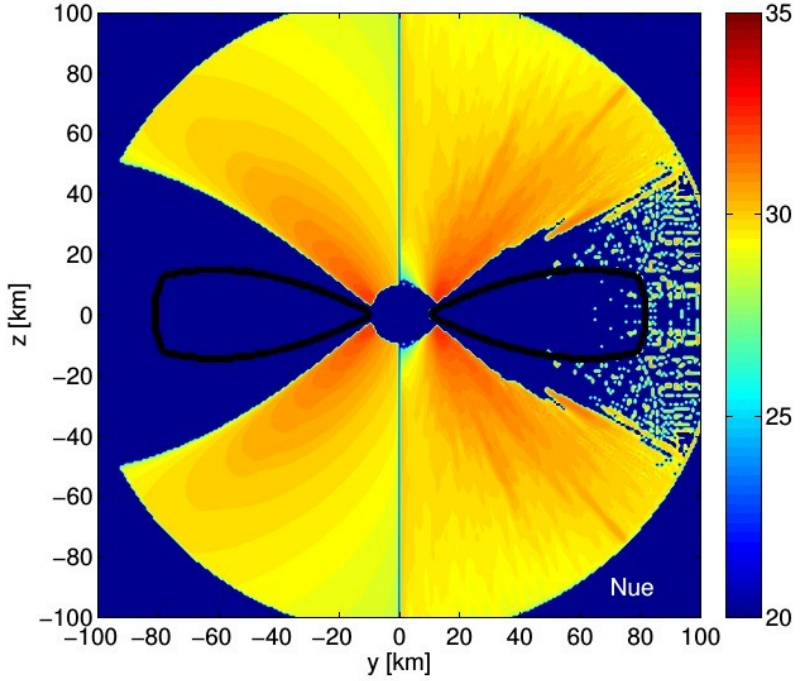

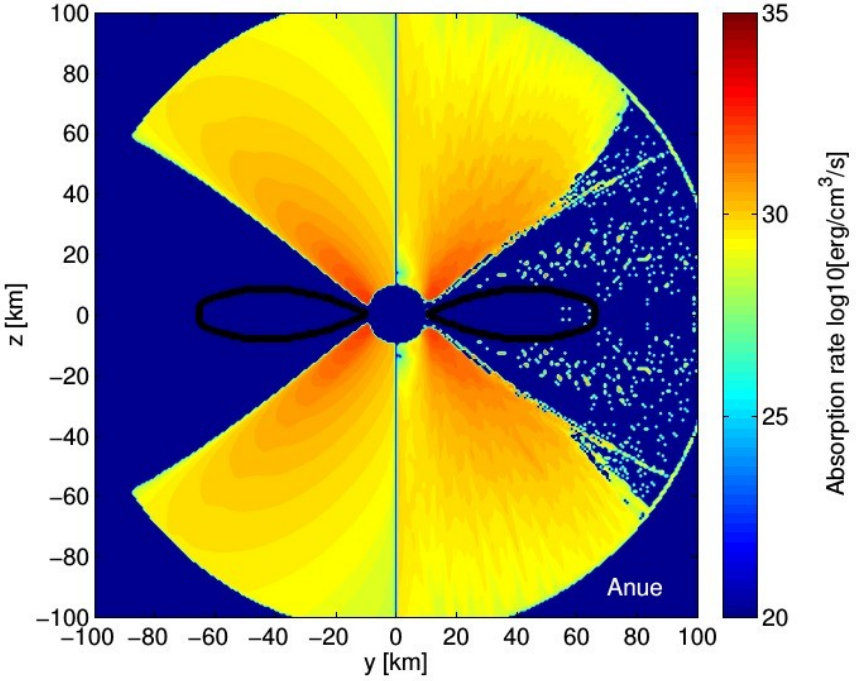

Outflows from Compact Binary Mergers

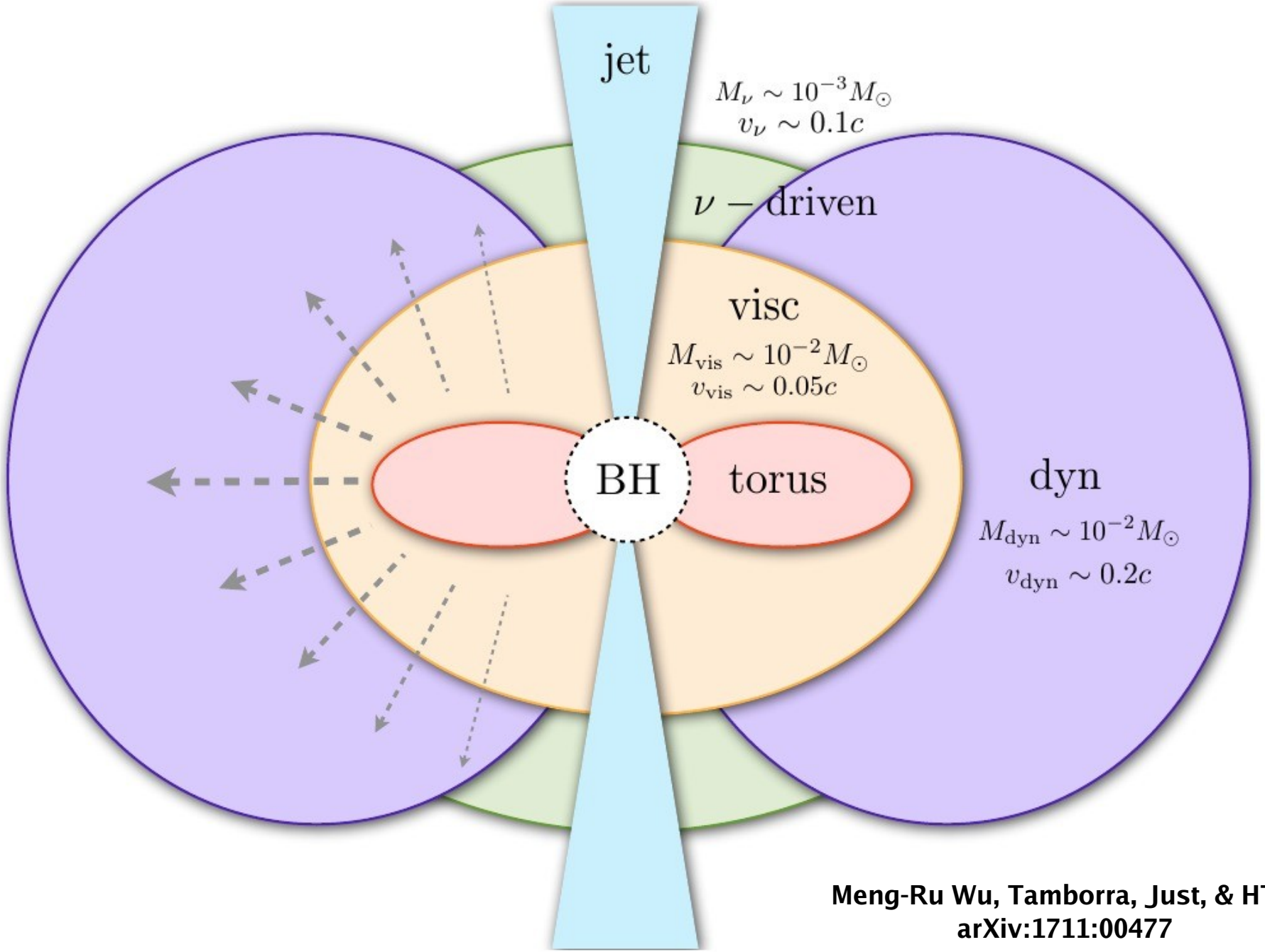

Meng-Ru Wu, Tamborra, Just, & HTJ,
arXiv:1711:00477

Dense Neutrinos in Neutron-Star Mergers

Non-Linear Equation of Motion for Neutrino Flavor:

Liouville equation for 3×3 occupation-number matrices in flavor space

$$\left(\partial_t + \vec{v}\cdot\vec{\nabla}\right)\varrho(t,\vec{r},\vec{p}) = -\mathrm{i}\,[\mathcal{H}(t,\vec{x},\vec{p}),\varrho(t,\vec{x},\vec{p})] + \mathcal{C}[\varrho(t,\vec{x},\vec{p})]$$

(Free streaming: collision term = 0)

Flavor evolution governed by "Hamiltonian matrix", for 2 flavors:

$$\mathcal{H} = \underbrace{\frac{\Delta m^2}{4E}\begin{pmatrix}\cos 2\theta & \sin 2\theta \\ \sin 2\theta & -\cos 2\theta\end{pmatrix}}_{\text{Vacuum oscillations}} + \underbrace{\sqrt{2}G_{\mathrm{F}}\begin{pmatrix}n_e & 0 \\ 0 & 0\end{pmatrix}}_{\text{MSW effect}} + \underbrace{\sqrt{2}G_{\mathrm{F}}\int\frac{d^3\vec{p}}{(2\pi)^3}(\varrho+\overline{\varrho})}_{\text{Nu-nu interaction term}}$$

Nu-nu interaction term
Nu's feed back on each other

- **Collective flavor modes of interacting system include "run-away" solutions**
- **Correspond to pairwise "fast flavor conversion"** $\nu_e + \overline{\nu}_e \rightarrow \nu_x + \overline{\nu}_x$
- **Much shorter length scales (order 10 cm) than usual (non-forward) pair processes**
- **Equilibrate flavor in NS-mergers and/or core-collapse SNe?**

Izaguirre, Raffelt & Tamborra, PRL 118 (2017) 021101; Meng-Ru Wu, Tamborra, Just, & HTJ, arXiv:1711:00477

Summary

- Enormous diversity of phenomena in NS-NS/BH mergers
- Dependent on many degrees of freedom:
  total system mass, mass ratio, spins, nuclear EoS
- Large sets of models needed!
- One observed event is not enough to learn all about mergers; don't generalize too quickly!
- Dynamical ejecta: < 0.02–0.03 Msun
  Secular (remnant) ejecta: can be even more
- Y_e and its phase and directional dependence are uncertain
- More work is needed on the complex neutrino physics